Supported by ERC through Starting Grant no. 759253

European Research Council
Established by the European Commission

Neutron star mergers and the high-density equation of state

International School of Nuclear Physics

The Strong Interaction: From Quarks and Gluons to Nuclei and Stars

Erice, 23/09/2018

Andreas Bauswein

(GSI Darmstadt)

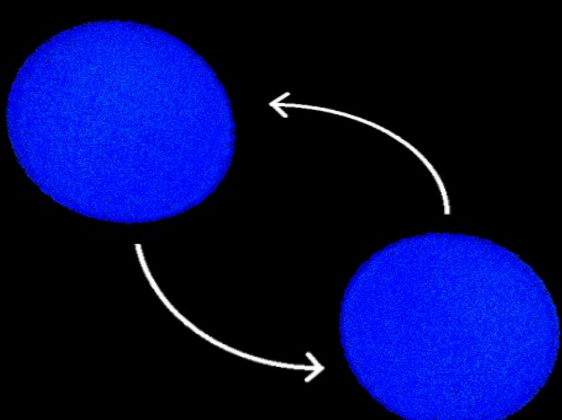

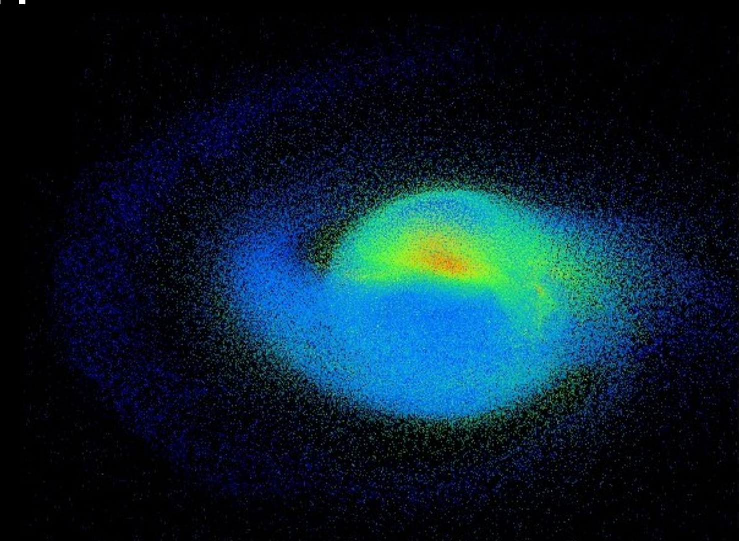

Outline

Focus of this talk on EoS impact / constraints

- Overview / introduction
- Simulations and ejecta masses
- Tidal deformability
- Collapse behavior
- NS radius constraints from GW170817
- dominant postmerger GW emission

  → NS radius measurements

  → maximum mass and other EoS constraints
- Signatures of the QCD phase transition

presence

future

A break-through in astrophysics

- GW170817 first unambiguously detected NS merger
- Mutli-messenger observations: gravitational waves, gamma, X-rays, UV, optical, IR, radio

Detection August 17, 2017 by LIGO-Virgo network

→ GW data analysis

→ follow-up observations - probably largest coordinated observing campaign in astronomy (observations/time)

Announcement October 2017

Scientific aspects of NS mergers

- NS mergers likely progenitors of short gamma-ray bursts (observed since the 70ies)
- NS mergers as sources of heavy elements forged by the rapid neutron-capture process
- Electromagnetic transient powered by nuclear decays during/after r-process ("kilonova", "macronova", ...)

  → UV, optical, IR → targets for triggered or blind searches (time-domain astronomy)
- Various other types of em counterparts
- Strong emitters of GWs

  → population properties: rates, masses, ... → stellar astrophysics

  → EoS of nuclear matter / stellar properties of NSs

  (NS mergers probe cold and hot matter – pre- and post-merger)
- ...

Dynamics

Inspiral of NS binary

~100 Myrs

Neutron star merger

dependent on EoS, M_{tot}

ms

Prompt formation of a BH + torus

ms

Formation of a differentially rotating massive NS

dependent on EoS, M_{tot}

Rigidly rotating (supermassive) NS

10-100 ms

Delayed collapse to a BH + torus

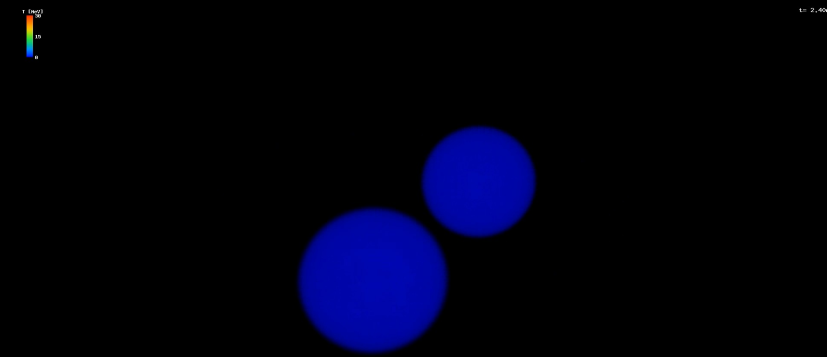

Dynamics

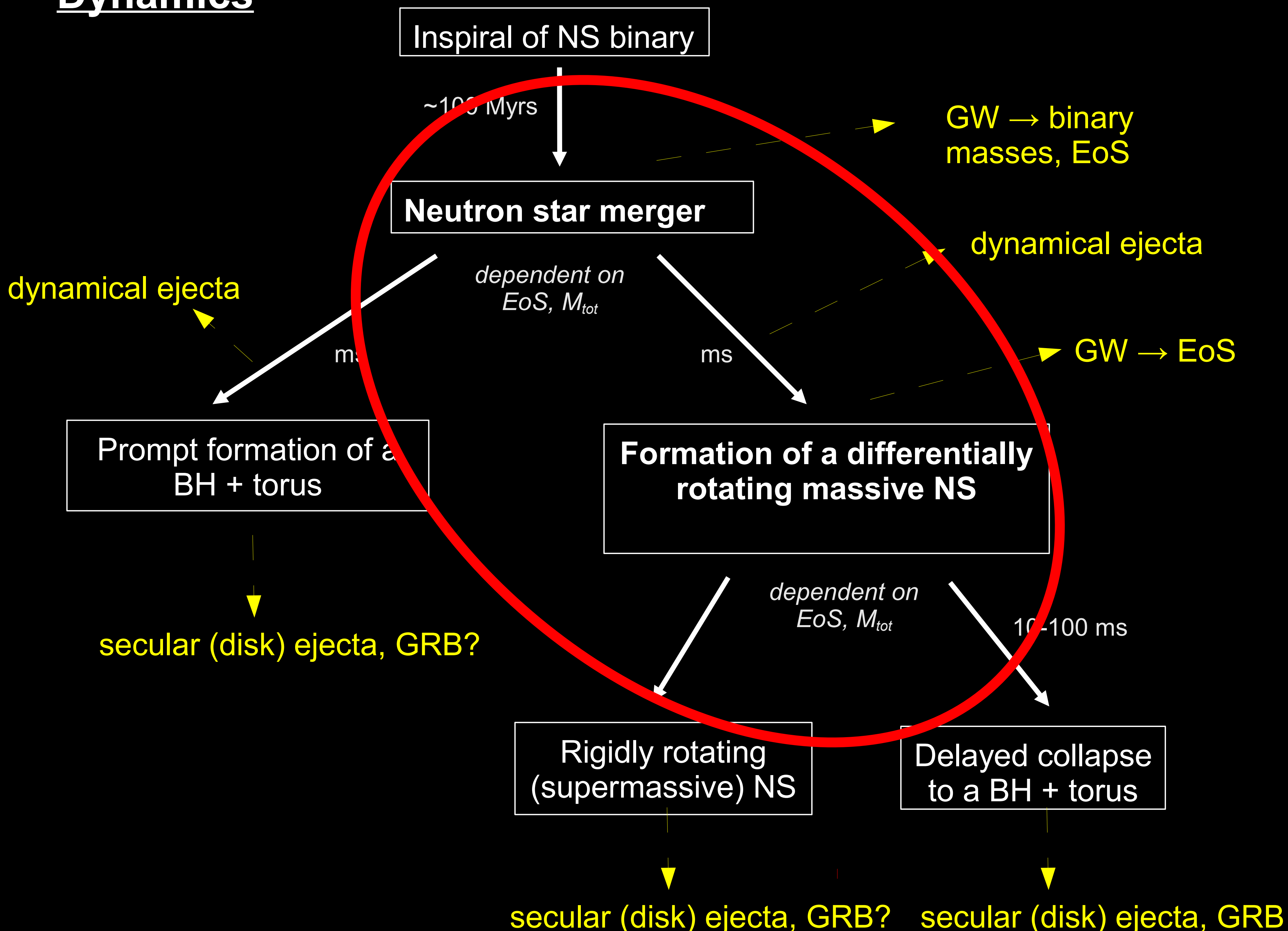

Inspiral of NS binary
~100 Myrs
GW → binary masses, EoS
Neutron star merger
dependent on EoS, M_{tot}
dynamical ejecta
dynamical ejecta
ms
ms
GW → EoS
Prompt formation of a BH + torus
Formation of a differentially rotating massive NS
secular (disk) ejecta, GRB?
dependent on EoS, M_{tot}
10-100 ms
Rigidly rotating (supermassive) NS
Delayed collapse to a BH + torus
secular (disk) ejecta, GRB?
secular (disk) ejecta, GRB

GW170817

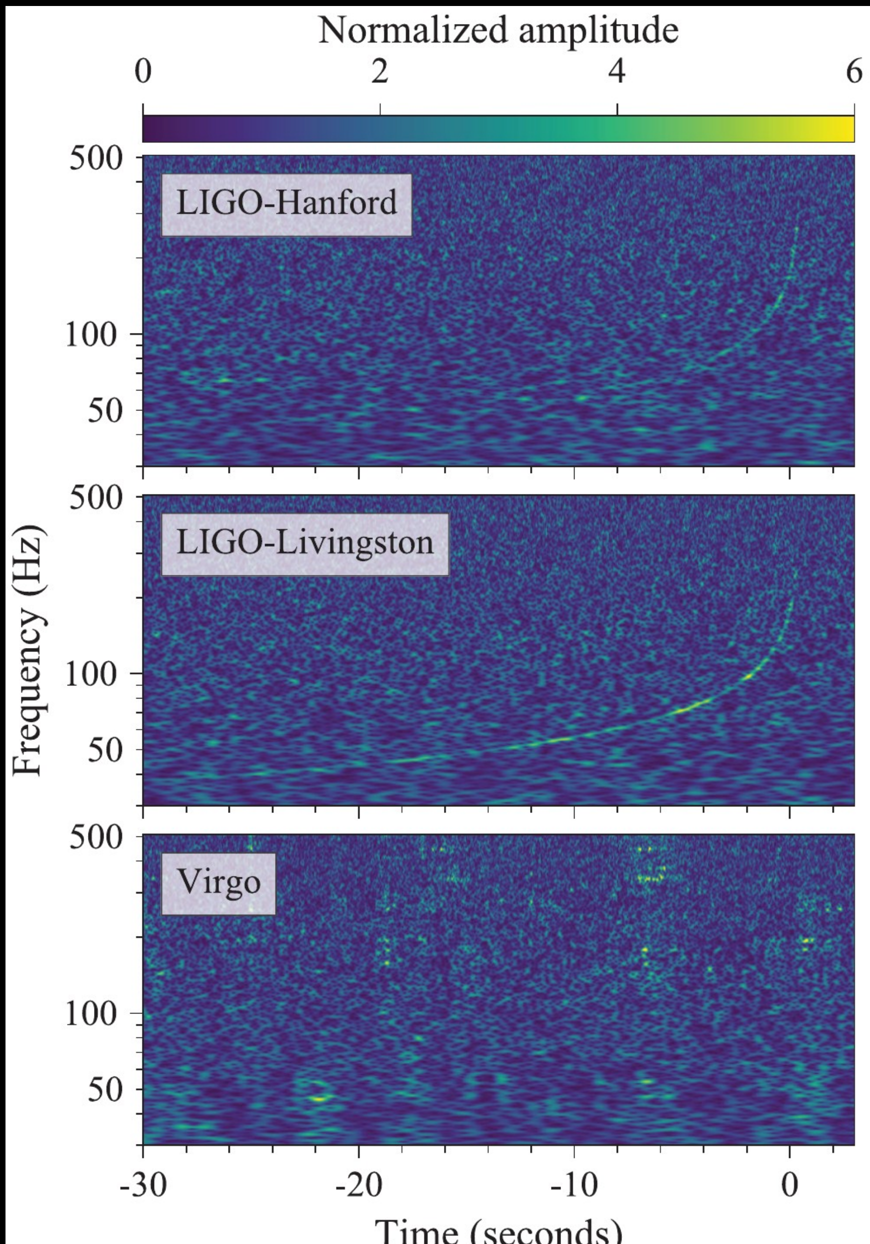

	Low-spin priors ($|\chi| \leq 0.05$)
Primary mass m_1	1.36–1.60 $M_\odot$
Secondary mass m_2	1.17–1.36 $M_\odot$
Chirp mass $\mathcal{M}$	$1.188^{+0.004}_{-0.002} M_\odot$
Mass ratio m_2/m_1	0.7–1.0
Total mass $m_{\rm tot}$	$2.74^{+0.04}_{-0.01} M_\odot$
Radiated energy $E_{\rm rad}$	$> 0.025 M_\odot c^2$
Luminosity distance $D_{\rm L}$	40^{+8}_{-14} Mpc
Viewing angle Θ	$\leq 55°$
Using NGC 4993 location	$\leq 28°$
Combined dimensionless tidal deformability $\tilde{\Lambda}$	≤ 800
Dimensionless tidal deformability $\Lambda(1.4 M_\odot)$	≤ 800

Chirp-like signal → compact binary merger

Shape reveals masses → only compatible with NSs

→ triggered some follow-up observations

Abbott et al 2017

Some insights from GW170817

- Binary masses measured from “inspiral” (= pre-merger phase with shrinking orbit)
- Detection at 40 Mpc → rate is presumably high !
- Note: chirp mass accurately measured
- Mass ratio only at higher PN order

$$\mathcal{M}_{chirp} = \frac{(M_1 M_2)^{3/5}}{(M_1 + M_2)^{1/5}} \qquad q = M_1/M_2$$

Abbott et al. 2017

	Low-spin priors ($\lvert\chi\rvert \leq 0.05$)	High-spin priors ($\lvert\chi\rvert \leq 0.89$)
Primary mass m_1	1.36–1.60 $M_\odot$	1.36–2.26 $M_\odot$
Secondary mass m_2	1.17–1.36 $M_\odot$	0.86–1.36 $M_\odot$
Chirp mass $\mathcal{M}$	$1.188^{+0.004}_{-0.002} M_\odot$	$1.188^{+0.004}_{-0.002} M_\odot$
Mass ratio m_2/m_1	0.7–1.0	0.4–1.0
Total mass $m_{\rm tot}$	$2.74^{+0.04}_{-0.01} M_\odot$	$2.82^{+0.47}_{-0.09} M_\odot$
Radiated energy $E_{\rm rad}$	$> 0.025 M_\odot c^2$	$> 0.025 M_\odot c^2$
Luminosity distance $D_{\rm L}$	40^{+8}_{-14} Mpc	40^{+8}_{-14} Mpc
Viewing angle Θ	$\leq 55°$	$\leq 56°$
Using NGC 4993 location	$\leq 28°$	$\leq 28°$
Combined dimensionless tidal deformability $\tilde{\Lambda}$	≤ 800	≤ 700
Dimensionless tidal deformability $\Lambda(1.4 M_\odot)$	≤ 800	≤ 1400

Observations

- 1.7 sec after gamma-rays (→ short GRB ???)
- Follow up observation (UV, optical, IR) starting ~12 h after merger

  → ejecta masses, velocities, opacities
- Several days later X-rays, radio (ongoing)

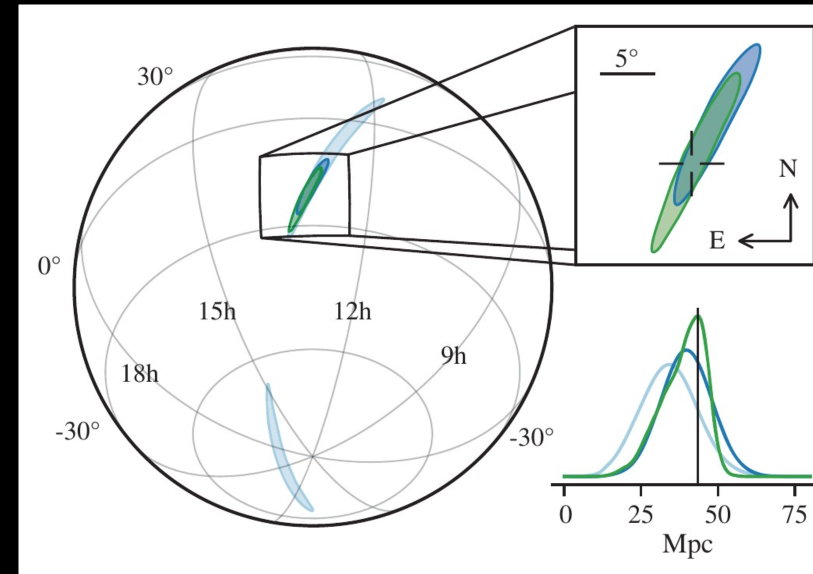

Abbott et al. 2017

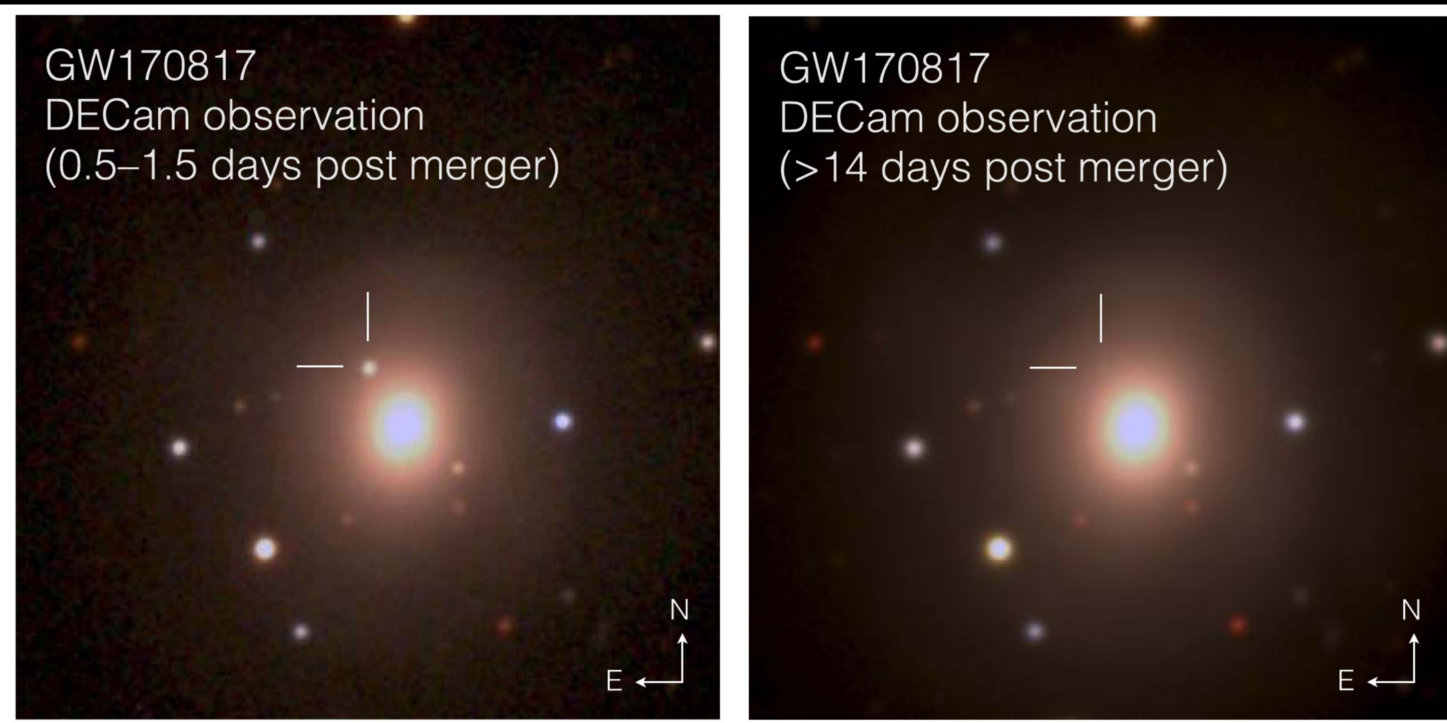

Figure 1. NGC4993 *grz* color composites (1.′5 × 1.′5). Left: composite of detection images, including the discovery *z* image taken on 2017 August 18 00:05:23 UT and the g and r images taken 1 day later; the optical counterpart of GW170817 is at R.A., decl. =197.450374, −23.381495. Right: the same area two weeks later.

Soares-Santos et al 2017

Observations

- Many IR/opt/UV observations by many groups
- Different interpretations / modeling
- Red and blue component
- Spectral features?
- Derived total ejecta masses all in the range 0.03 … 0.05 Msun

Chronock et al. 2017, Levan & Tanvir 2017, Kasliwal et al. 2017, Coulter et al. 2017, Allam et al. 2017, Yang et al. 2017, Arcavi et al. 2017, Kilpatrick et al. 2017, McCully et al. 2017, Pian et al. 2017, Arcavi et al. 2017, Evans et al. 2017, Drout et al. 2017 Lipunov et al. 2017, Cowperthwaite et al. 2017, Smarrt et al. 2017, Shappee et al. 2017, Nicholl et al. 2017, Kasen et al. 2017, Tanaka et al. 2017, …..

Reference	$m_{\rm dyn}$ $[M_\odot]$	$m_{\rm w}$ $[M_\odot]$
Abbott et al. (2017a)	$0.001 - 0.01$	–
Arcavi et al. (2017)	–	$0.02 - 0.025$
Cowperthwaite et al. (2017)	0.04	0.01
Chornock et al. (2017)	0.035	0.02
Evans et al. (2017)	$0.002 - 0.03$	$0.03 - 0.1$
Kasen et al. (2017)	0.04	0.025
Kasliwal et al. (2017b)	> 0.02	> 0.03
Nicholl et al. (2017)	0.03	–
Perego et al. (2017)	$0.005 - 0.01$	$10^{-5} - 0.024$
Rosswog et al. (2017)	0.01	0.03
Smartt et al. (2017)	$0.03 - 0.05$	0.018
Tanaka et al. (2017a)	0.01	0.03
Tanvir et al. (2017)	$0.002 - 0.01$	0.015
Troja et al. (2017)	$0.001 - 0.01$	$0.015 - 0.03$

Compilation by Cote et al 2018

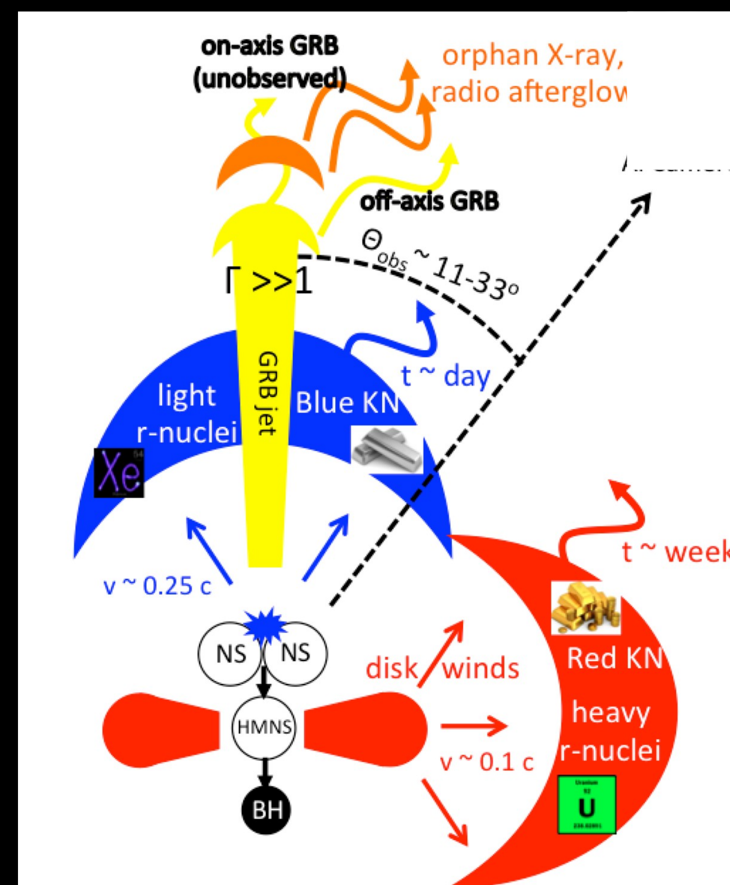

Metzger 2017

Interpretation - implications

- heating and derived opacities are compatible with r-processing ejecta !!!

  (not surprising for a theorist, see earlier work on r-process and em counterparts)

- Ejecta velocities and masses in ballpark of simulation results (→ later)

- Derived ejecta masses are compatible with mergers being the main source of heavy r-process elements in the Universe

  → overall strong evidence that NS mergers play a prominent role for heavy element formation

  see talk by Martinez-Pinedo

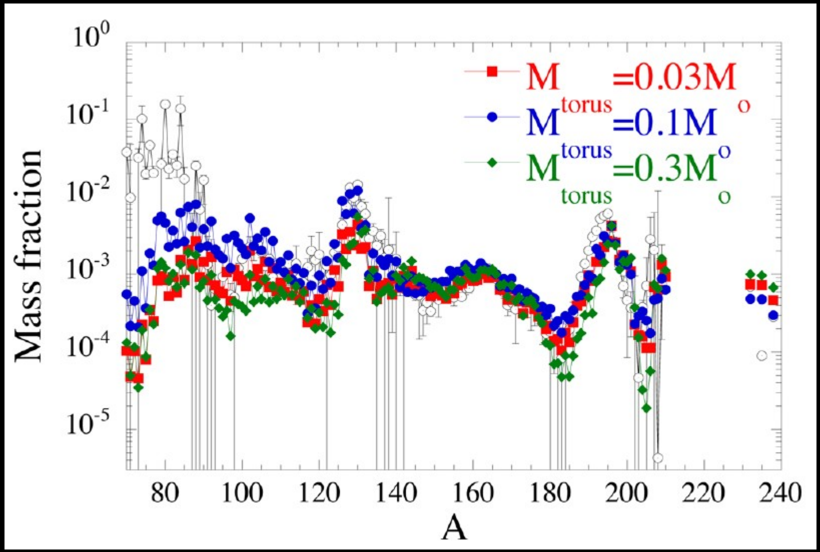

Just et al. 2015

Only A>130

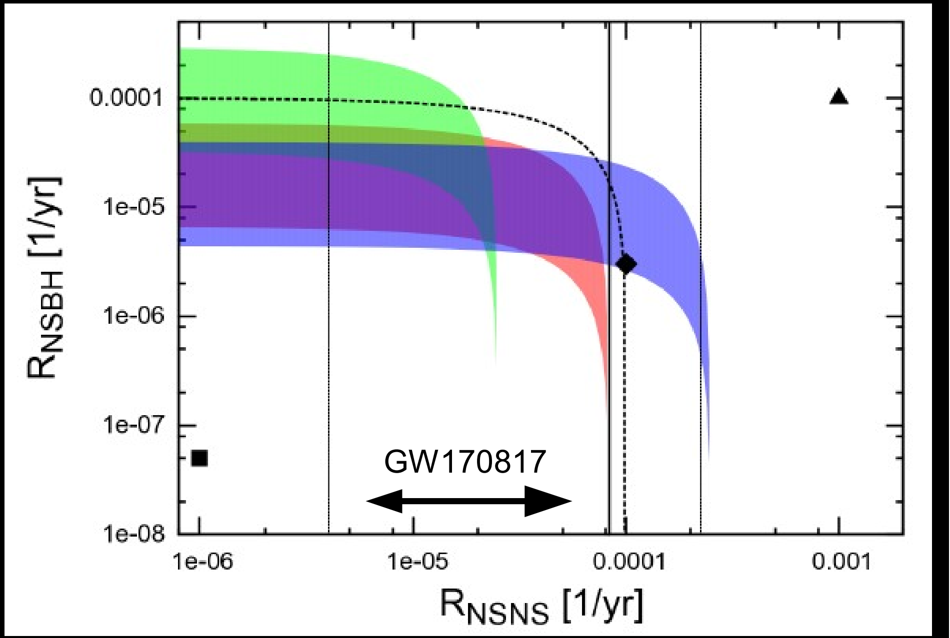

Bauswein et al. 2014

More insights

- Em counterpart allows association with host galaxy NGC 4993
- GW signal → luminosity distance

  + redshift of galaxy

  → independent estimate of Hubble constant
- Compatible with other estimates, e.g. Planck, SNe

EoS / NS constraints

Importance of EoS

- Understand properties of high-density matter (hardly accessible by laboratory experiments – theoretically challenging)

  → e.g. nuclear parameter/models (also important for nucleosynthesis models)

  → phase transition to hyperonic matter? Quark matter?

- Stellar properties of NS (observationally challenging)

  → EoS affects dynamics/phenomenology of mergers (e.g em counterparts, nucleosynthesis, GRBs), supernovae, NS cooling, ...

Finite-size effects during late inspiral

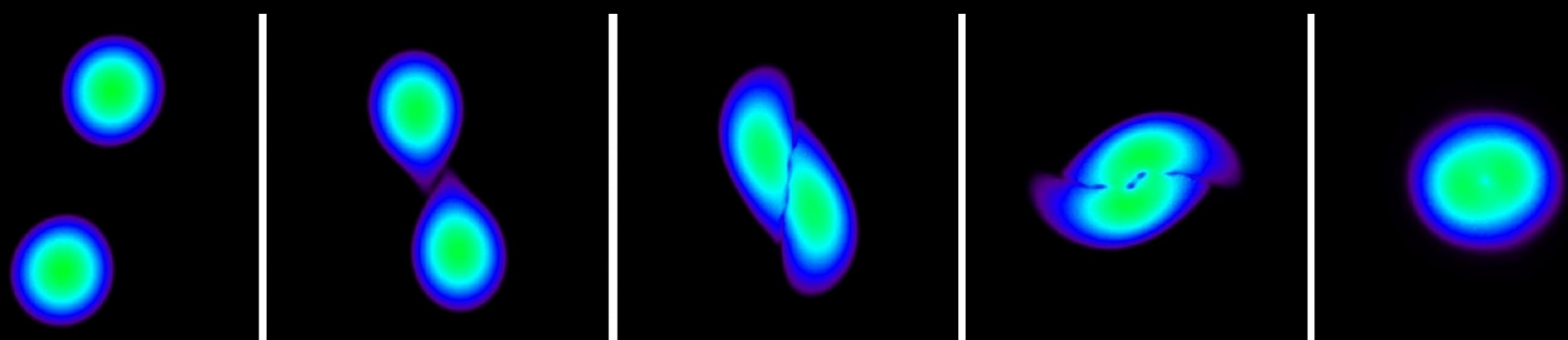

See Lattimer's talk

Description of tidal effects during inspiral

- Tidal field E_{ij} of on star induces change of quadrupole moment Q_{ij} of other component
- Changed quadrupole moment affects GW signal, especially phase evolution

  → inspiral faster compared to point-particle inspiral
- Strength of induced quadrupole moment depends on NS structure / EoS:

$$Q_{ij} = -\lambda(M)\, E_{ij} \qquad \lambda(M) = \frac{2}{3} k_2(M) R^5$$

- Tidal deformability depends on radius (clear – smaller stars are harder to deform) and "Love number" k_2 (~"TOV" properties)
- k_2 also depends on EoS and mass

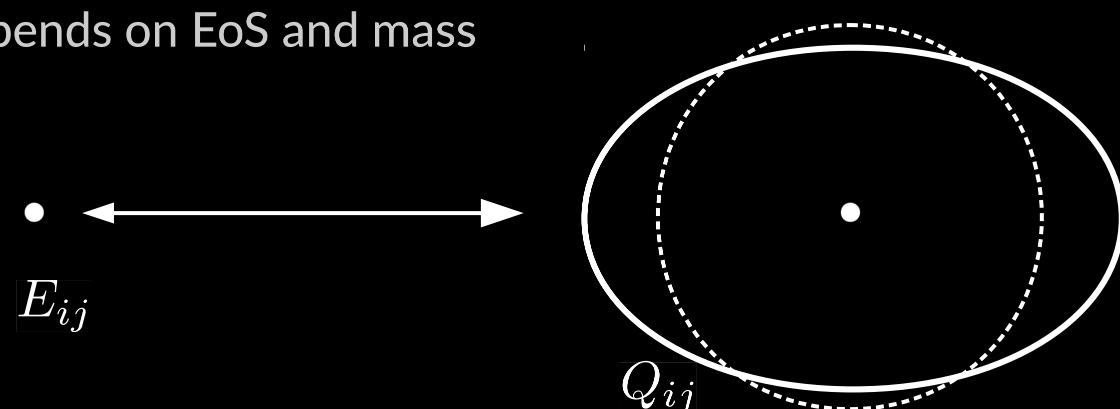

Inspiral

- Orbital phase evolution affected by tidal deformability – only during last orbits before merging
- Inspiral accelerated compared to point-particle inspiral for larger Lambda
- Difference in phase between NS merger and point-particle inspiral:

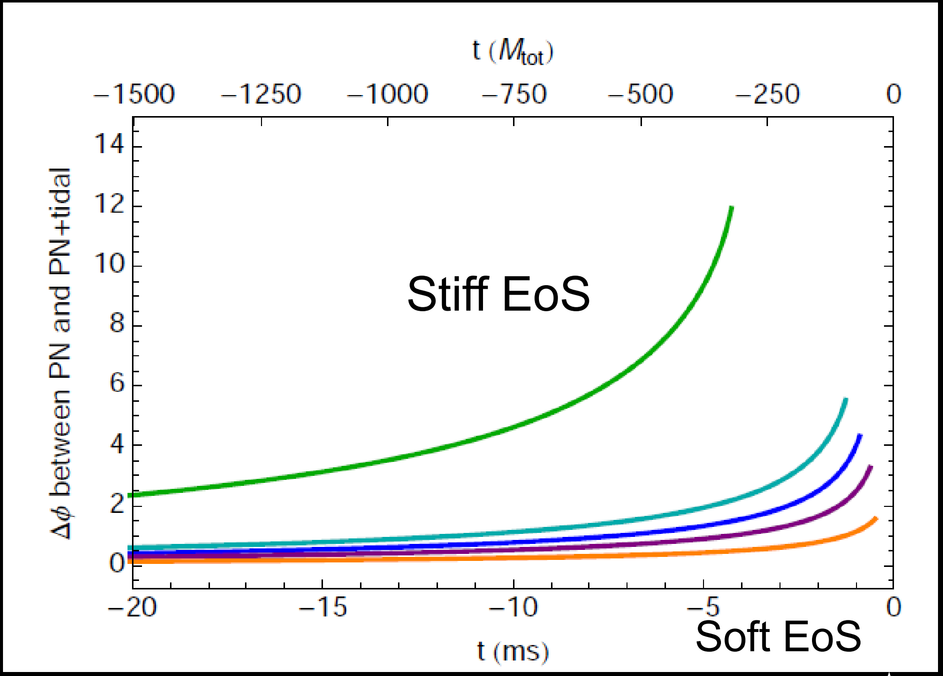

EoS impact measured by tidal deformability

$$\Lambda(M) = \frac{2}{3} k_2(M) \left(\frac{c^2 R}{G\,M} \right)^5$$

e.g. Read et al. 2013

Merger time of point particle

Challenge: construct faithful templates for data analysis

Measurement

- Lambda < ~800

  → Means that very stiff EoSs are excluded

- Recall uncertainties in mass measurements (only Mchirp accurate)

- systematic errors in waveform model

  → ongoing research

- Better constraints expected in future as sensitivity increases

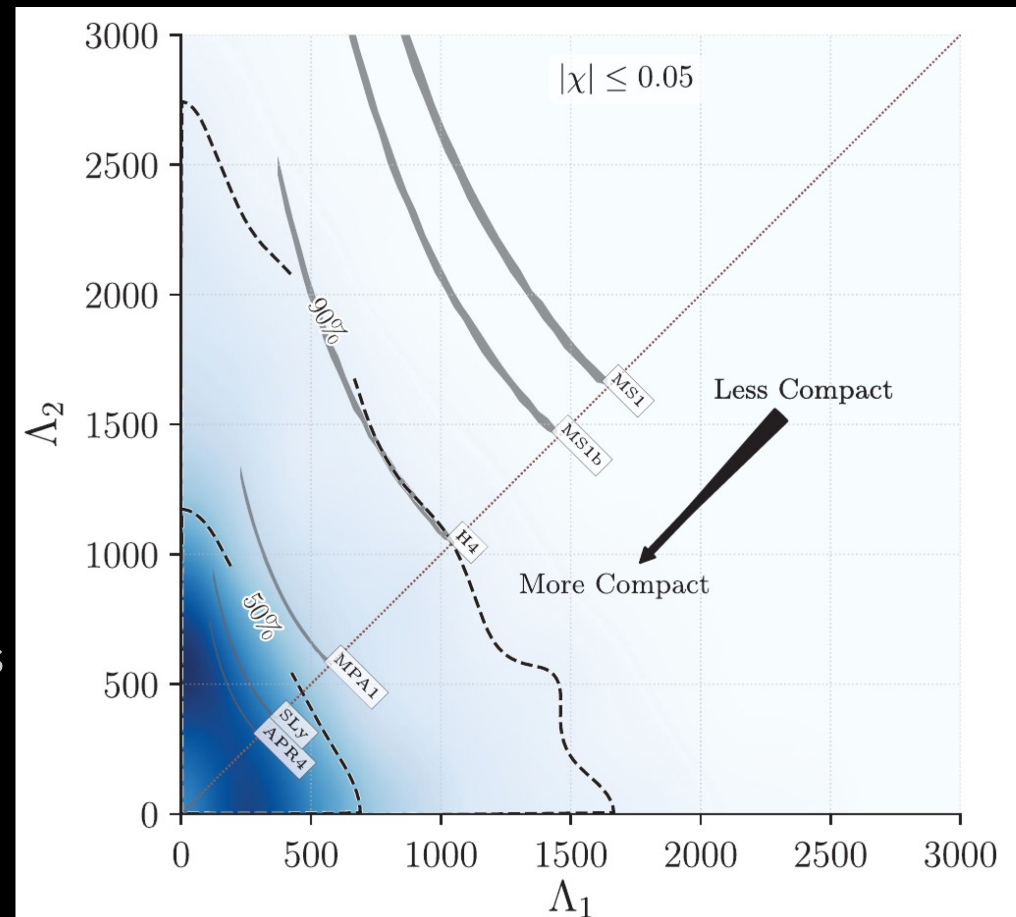

$$\tilde{\Lambda} = \frac{16}{13}\frac{(m_1 + 12m_2)m_1^4\Lambda_1 + (m_2 + 12m_1)m_2^4\Lambda_2}{(m_1 + m_2)^5}$$

Abbott et al. 2017
See also later publications by
Ligo/Virgo collaboration, De et al. 2018

See Lattimer's talk

- Combined tidal deformability vs. radius (for constant chirp mass)

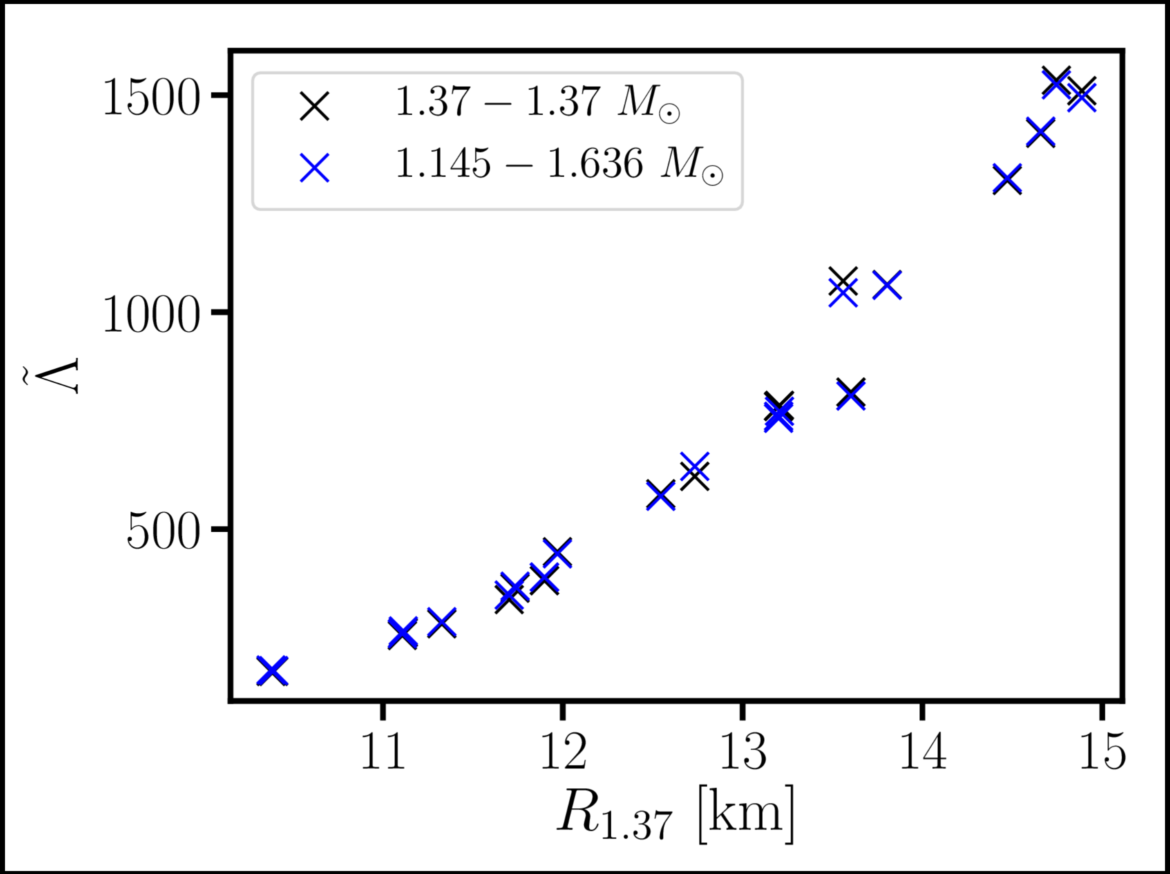

→ GW170817 constrains NS radii from above

Simulation results – ejecta

(EoS and binary mass dependence)

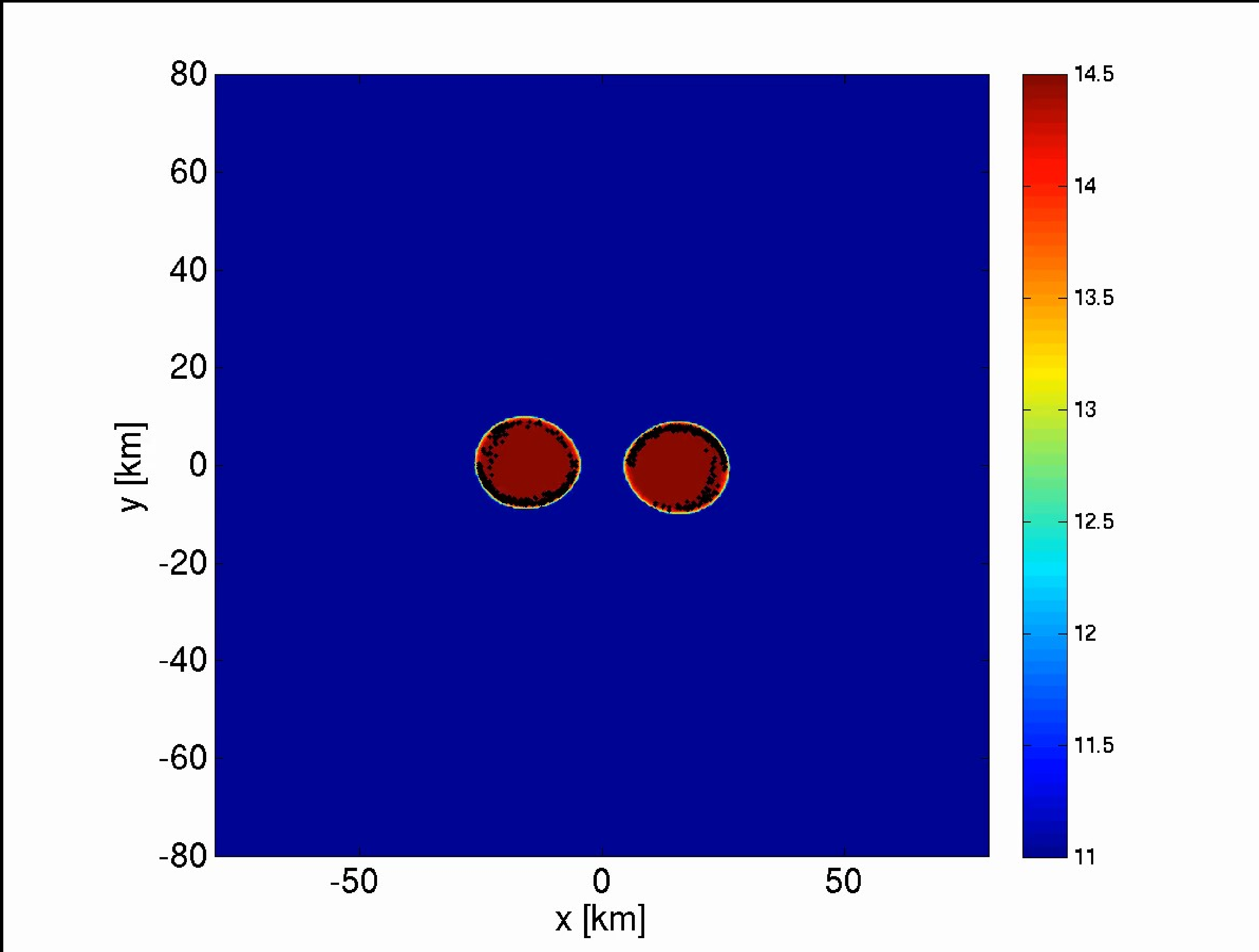

DD2 1.35-1.35 M_{sun}, representative ejecta particles (white unbound)

Simulations

Dots trace ejecta (DD2 EoS 1.35-1.35 M_{sun})

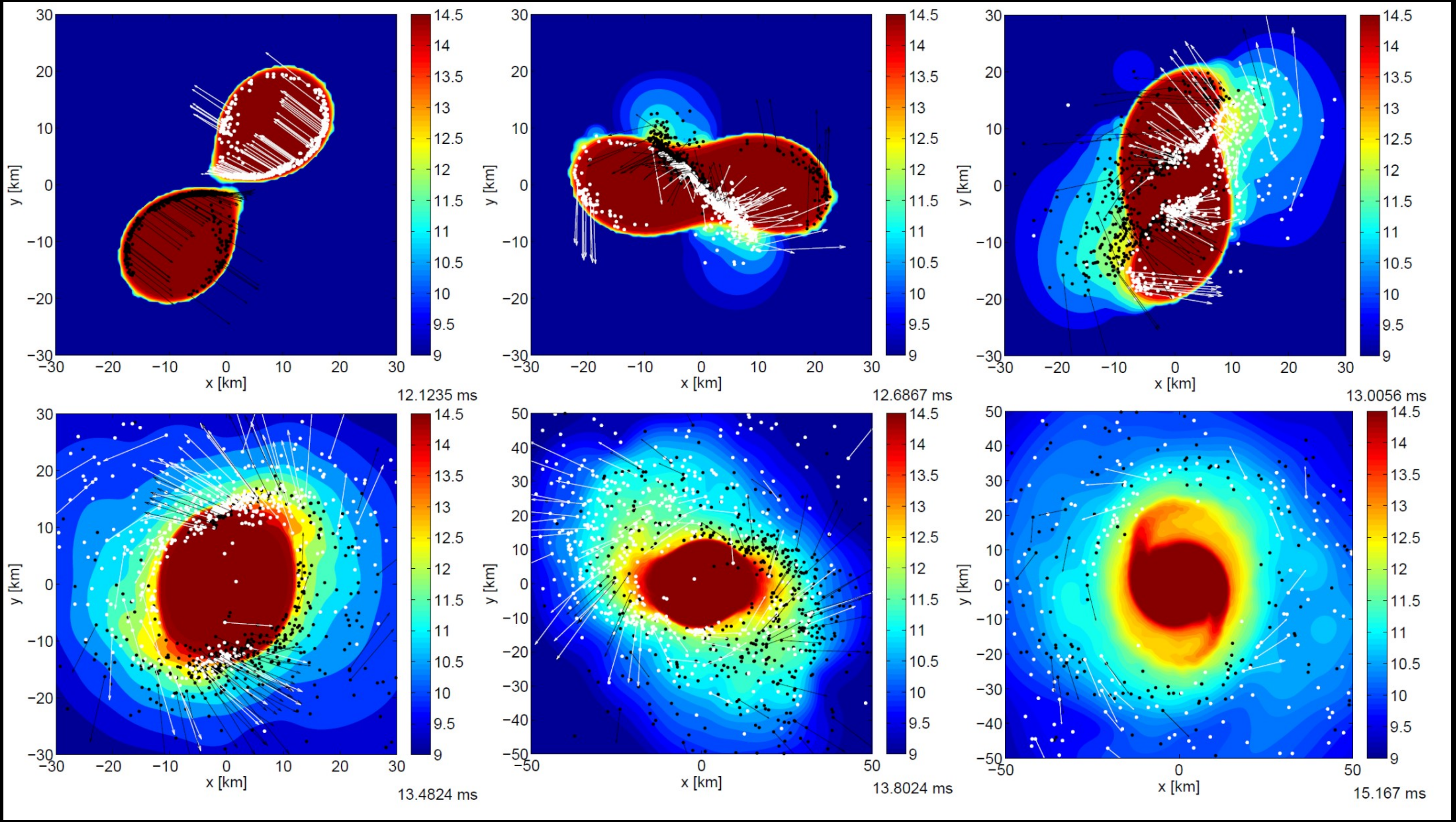

Bauswein et al. 2013

Asymmetric mergers

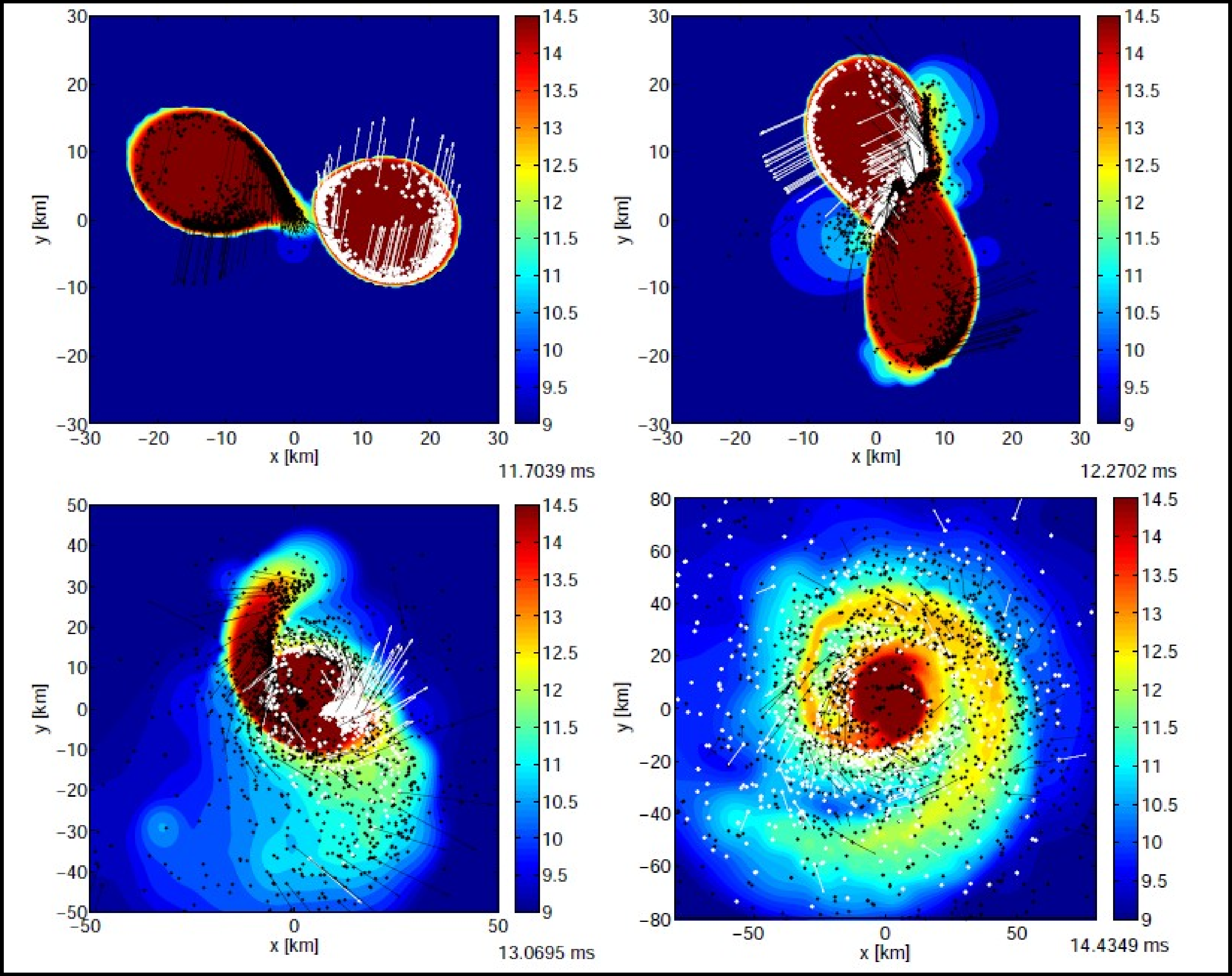

→ larger tidal component, larger total ejecta masses

Bauswein et al. 2013

Ejecta mass dependence

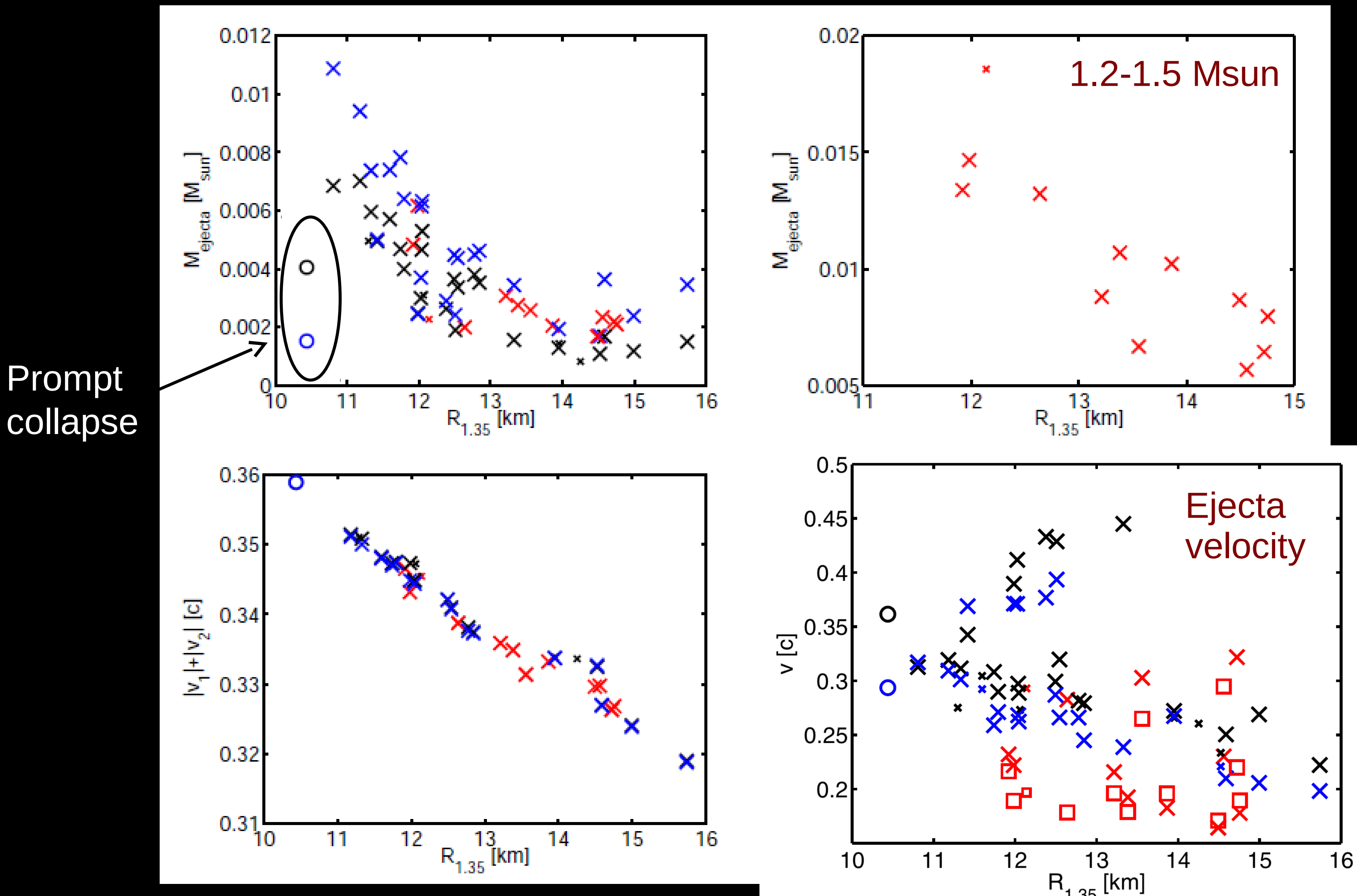

Different EoSs characterized by radii of 1.35 M_{sun} NSs (note importannce of thermal effects)

Coarse picture: EoS dependence of ejecta mass

- Ejecta mass 0.03-0.05 Msun in GW170817
- Excludes tentatively very stiff EoSs
- Excludes tentatively very soft EoSs – prompt collapse !!!

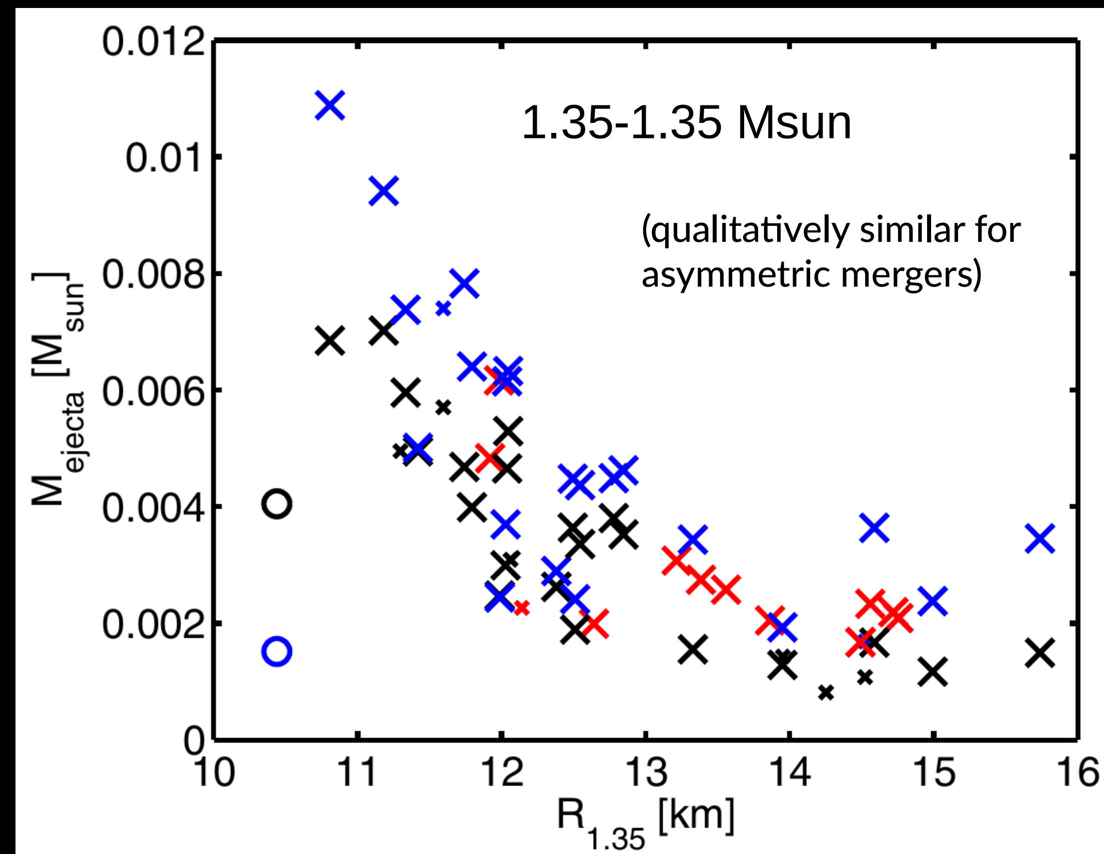

Bauswein et al 2013, see also Hotokezaka et al 2013

+ secular ejecta (viscous, neutrino)

Reference	$m_{\rm dyn}$ $[M_\odot]$	$m_{\rm w}$ $[M_\odot]$
Abbott et al. (2017a)	$0.001 - 0.01$	–
Arcavi et al. (2017)	–	$0.02 - 0.025$
Cowperthwaite et al. (2017)	0.04	0.01
Chornock et al. (2017)	0.035	0.02
Evans et al. (2017)	$0.002 - 0.03$	$0.03 - 0.1$
Kasen et al. (2017)	0.04	0.025
Kasliwal et al. (2017b)	> 0.02	> 0.03
Nicholl et al. (2017)	0.03	–
Perego et al. (2017)	$0.005 - 0.01$	$10^{-5} - 0.024$
Rosswog et al. (2017)	0.01	0.03
Smartt et al. (2017)	$0.03 - 0.05$	0.018
Tanaka et al. (2017a)	0.01	0.03
Tanvir et al. (2017)	$0.002 - 0.01$	0.015
Troja et al. (2017)	$0.001 - 0.01$	$0.015 - 0.03$

Compilation in Cote et al 2018

Ejecta mass dependencies: binary para.

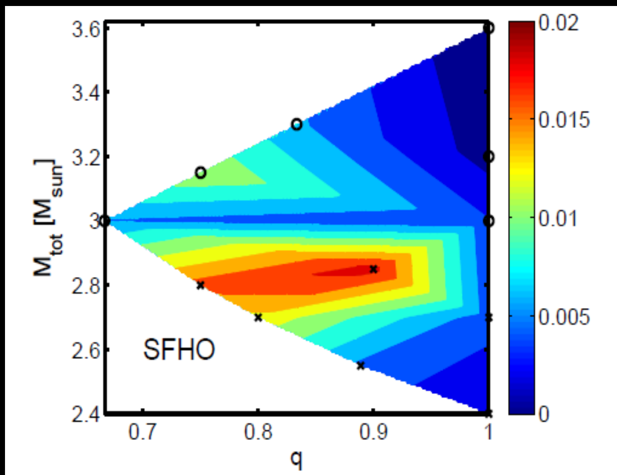

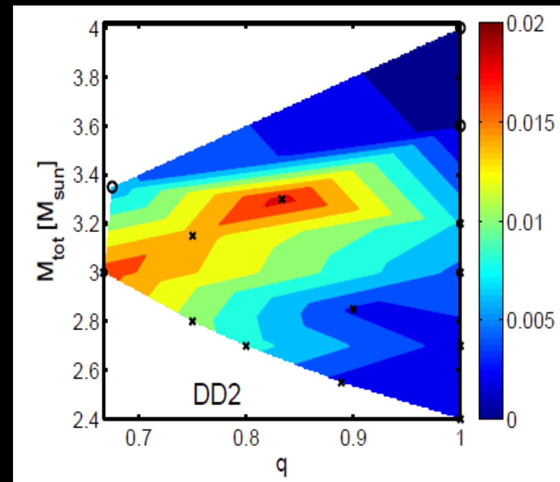

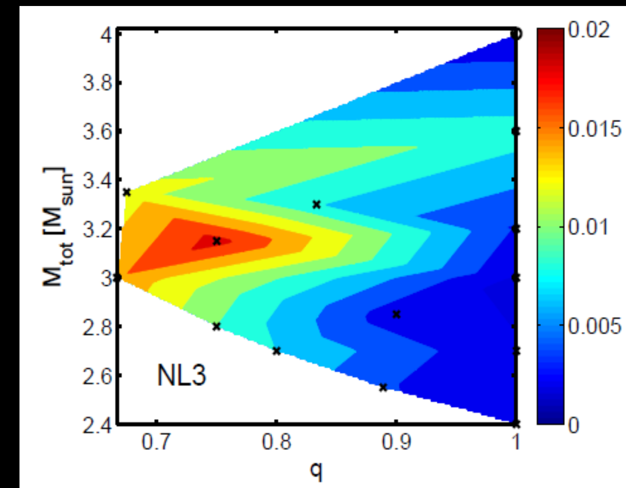

Stiffness

understandable by different dynamics / impact velocity / postmerger oscillations

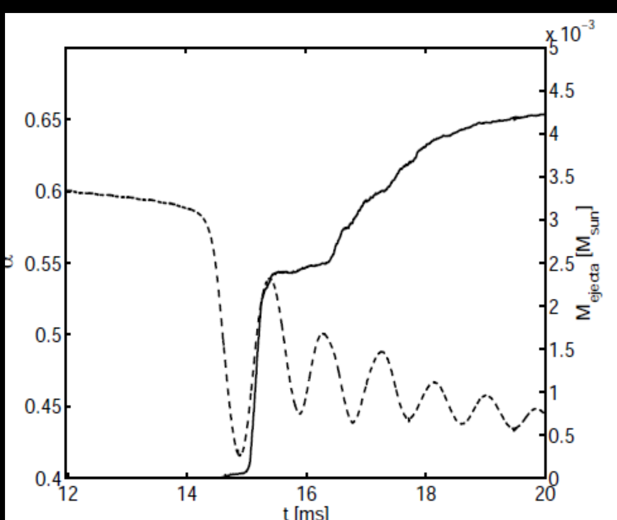

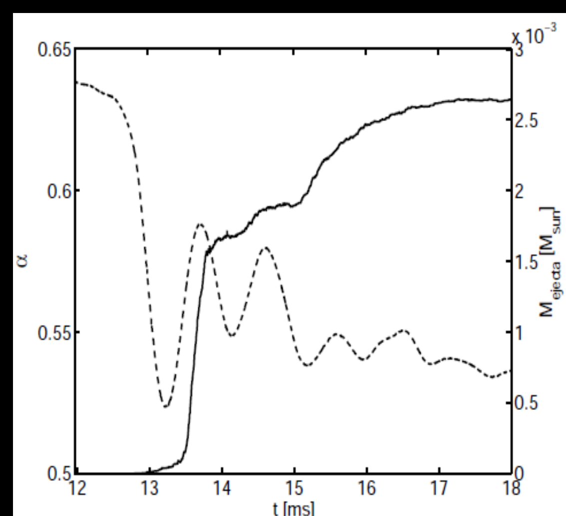

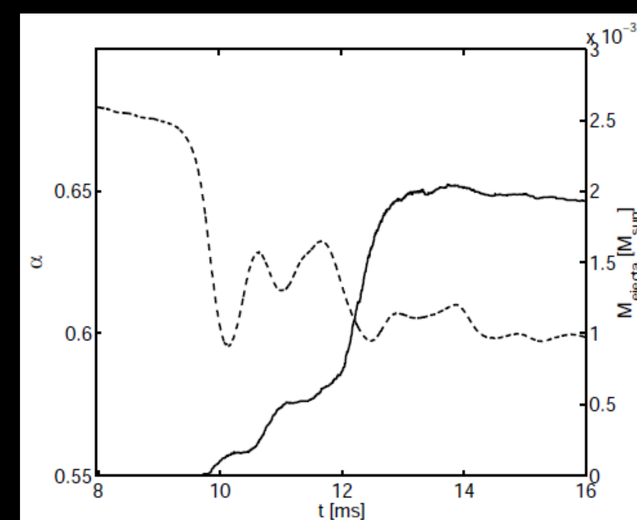

Central lapse α traces remnant compactness / oscillations / dynamics (dashed lines)

Secular and dynamical ejecta

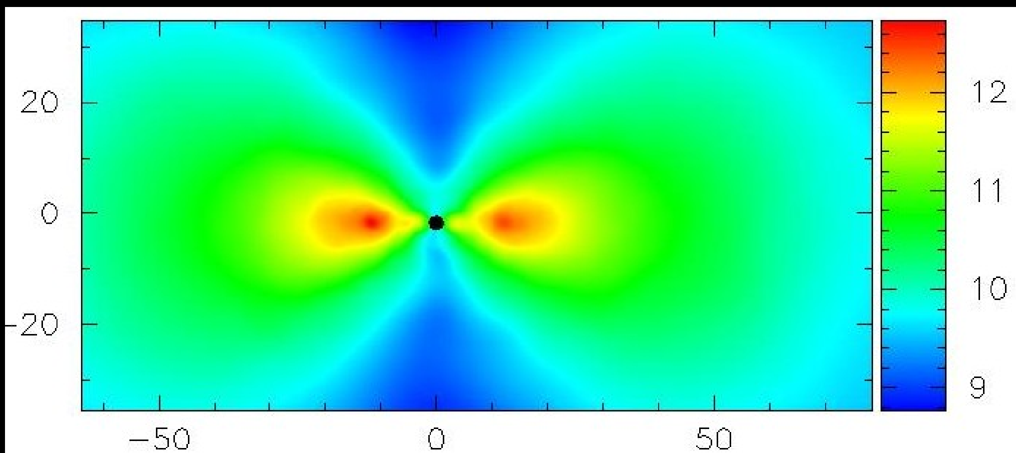

Just et al. 2015

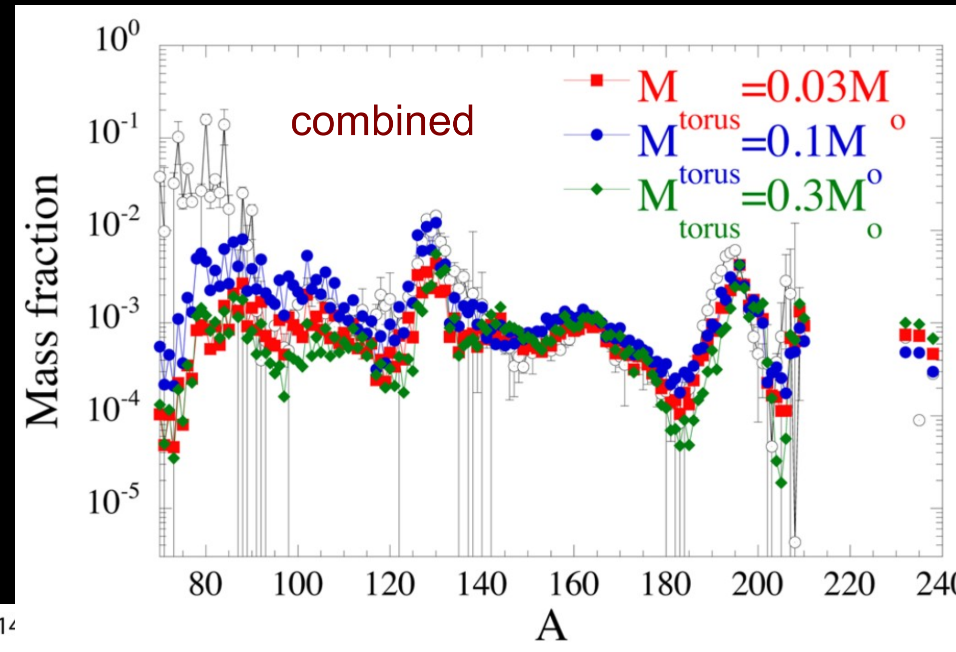

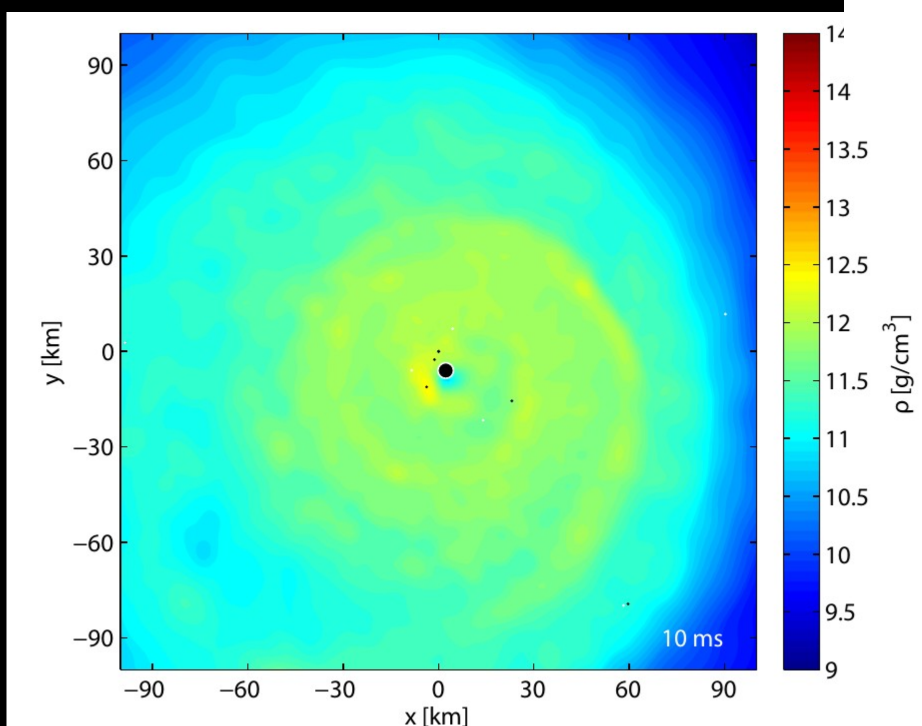

Wu et al. 2016, only secular ejecta

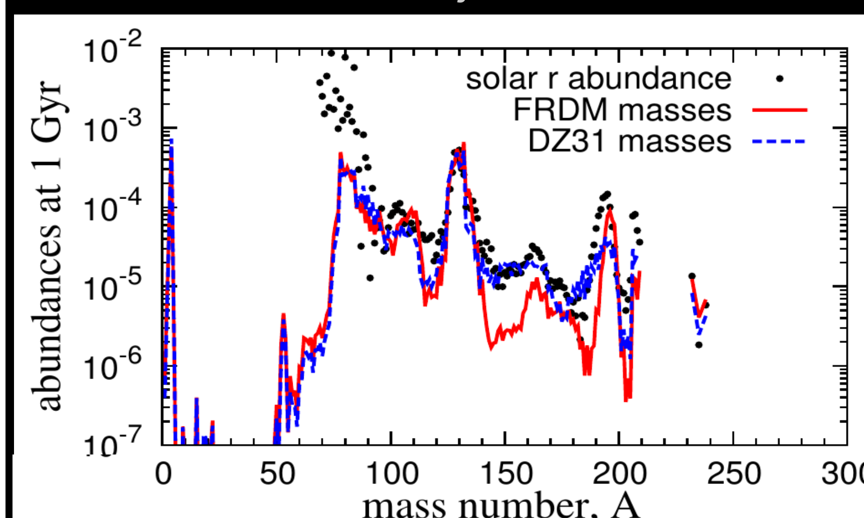

Secular ejecta

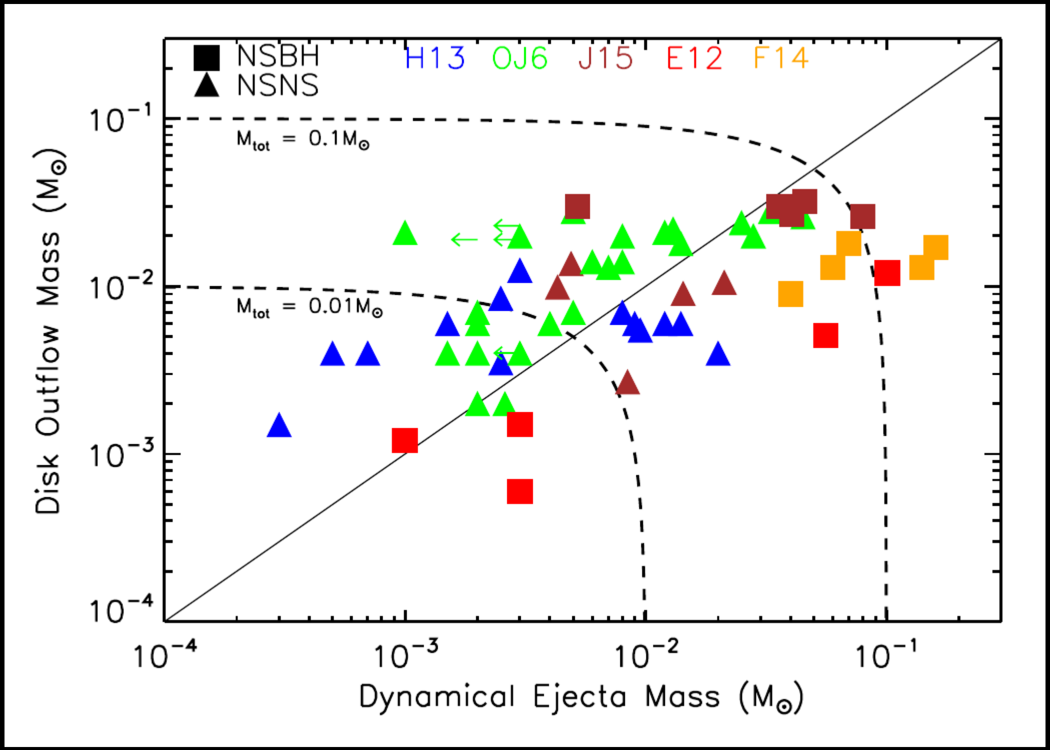

Wu et al. 2016

Typically several per cent of disk mass ejected (e.g. Fernandez et al. 2014, Perego et al. 2014, Just et al 2015) → production of light and heavy r-process elements, contributing to em counterpart

Considering only heavy elements with A > 140

=> not clear how much of this material in GW170817 !!!

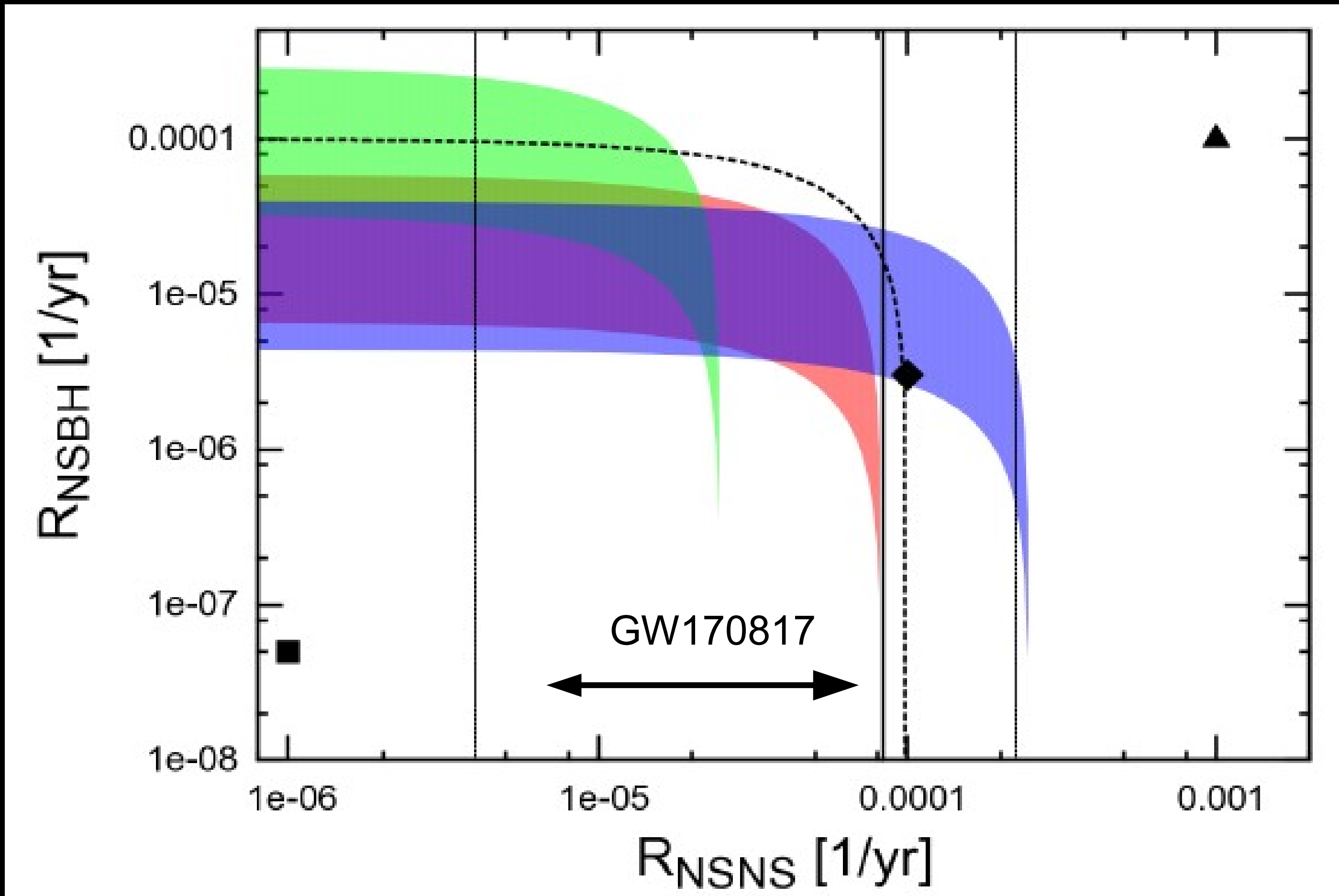

M_{ej}(NSNS):

Blue: 10^{-3} M_{sun}

Red: $3*10^{-3}$ M_{sun}

Green: 10^{-2} M_{sun}

- Colored bands: rates for different EoSs
- Symbols: population synthesis predictions (Abadie et al. 2010)
- Vertical lines: pulsar observations (Kalogera et al. 2004)
- Dashed curve: short GRBs (Berger 2013)
- Arrow: volumetric rate (Abbott et al. 20017) converted to Galactic rate

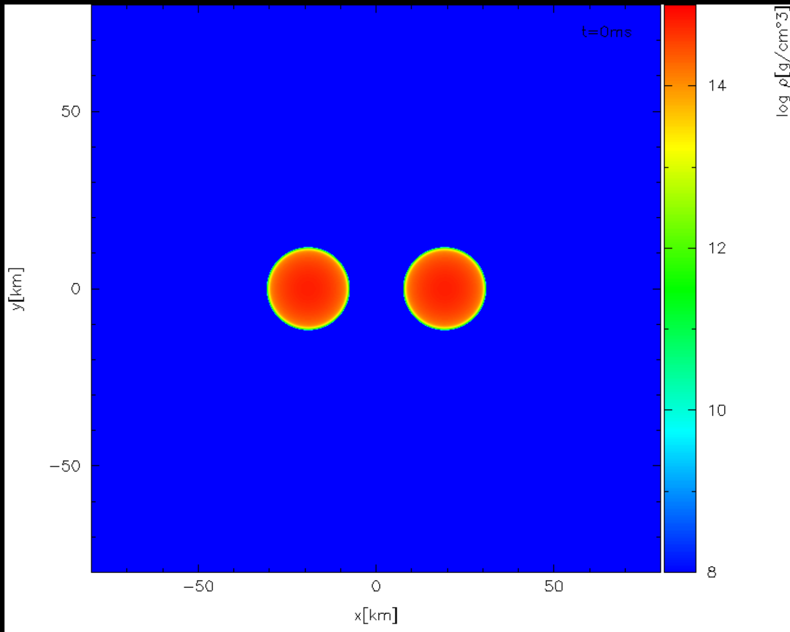

$$M_{\rm tot} = 3.4\ M_\odot$$

$$M_{\rm tot} = 3.5\ M_\odot$$

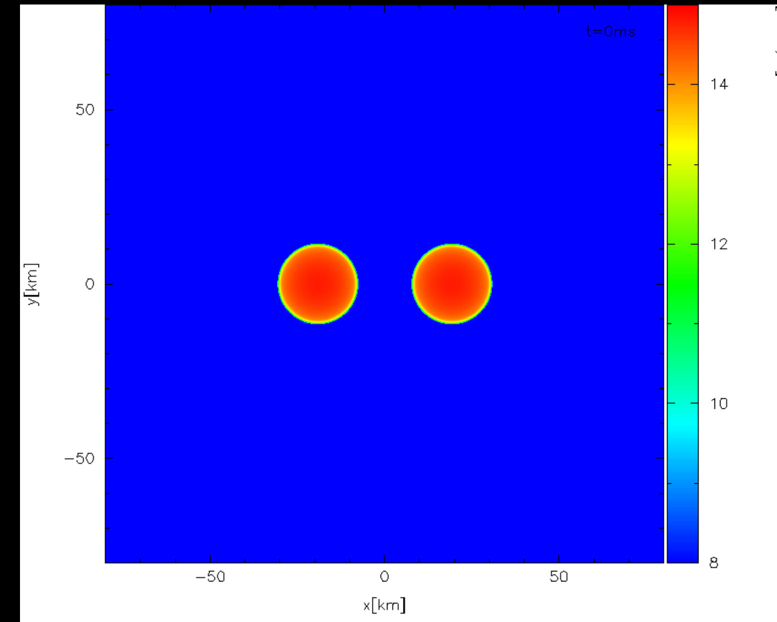

Shen EoS

Collapse behavior: Prompt vs. delayed (/no) BH formation

Relevant for:

EoS constraints through M_{max} measurement

Conditions for short GRBs

Mass ejection

Electromagnetic counterparts powered by thermal emission

And NS radius constraints !!!

Collapse behavior

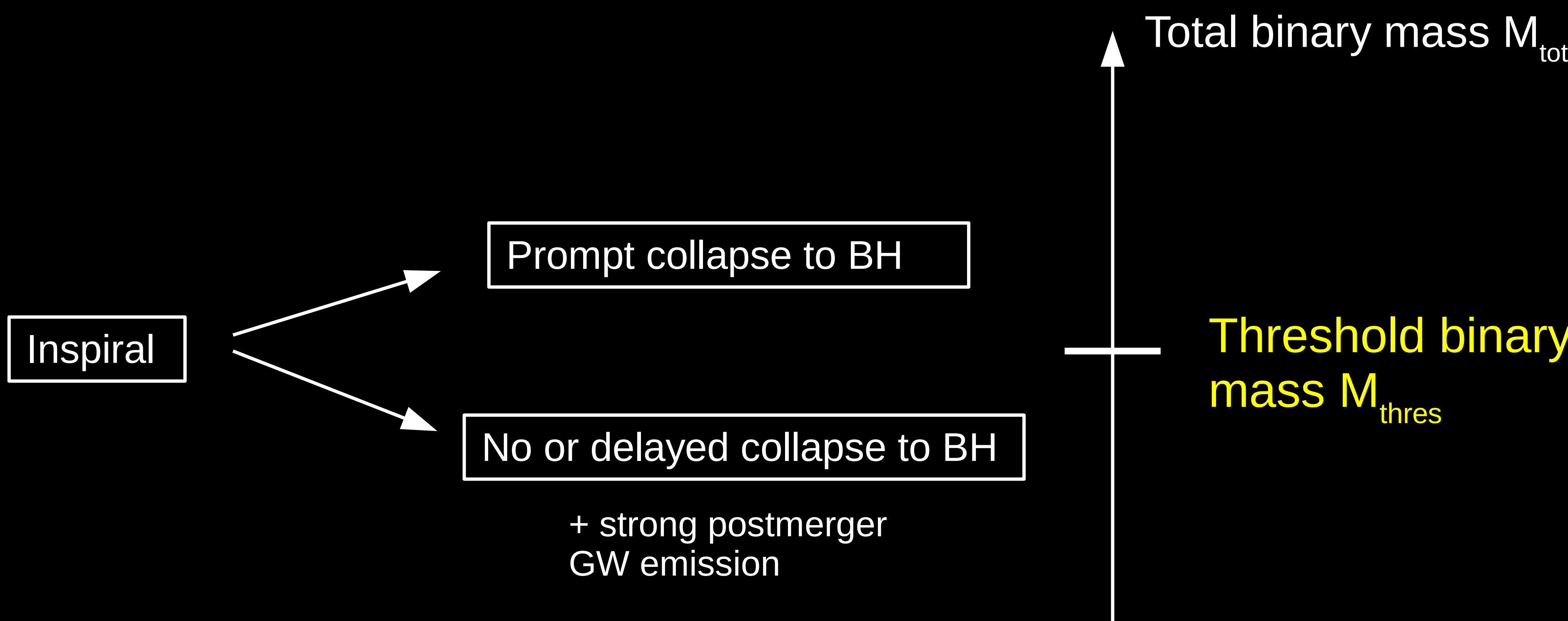

EoS dependent - somehow M_{max} should play a role

Simulations reveal M_{thres}

TOV properties of nonrotating stars, i.e. EoS characteristics

Merger property from simulations

EoS	M_{max} ($M_\odot$)	R_{max} (km)	C_{max}	$R_{1.6}$ (km)	M_{thres} ($M_\odot$)
NL3 [37,38]	2.79	13.43	0.307	14.81	3.85
GS1 [39]	2.75	13.27	0.306	14.79	3.85
LS375 [40]	2.71	12.34	0.325	13.71	3.65
DD2 [38,41]	2.42	11.90	0.300	13.26	3.35
Shen [42]	2.22	13.12	0.250	14.46	3.45
TM1 [43,44]	2.21	12.57	0.260	14.36	3.45
SFHX [45]	2.13	10.76	0.292	11.98	3.05
GS2 [46]	2.09	11.78	0.262	13.31	3.25
SFHO [45]	2.06	10.32	0.294	11.76	2.95
LS220 [40]	2.04	10.62	0.284	12.43	3.05
TMA [44,47]	2.02	12.09	0.247	13.73	3.25
IUF [38,48]	1.95	11.31	0.255	12.57	3.05

Bauswein et al. 2013

Smooth particle hydrodynamics + conformal flatness

Threshold binary mass

- Empirical relation from simulations with different M_{tot} and EoS
- Fits (to good accuracy):

$$M_{\rm thres} = M_{\rm thres}(M_{\rm max}, R_{\rm max}) = \left(-3.38\frac{GM_{\rm max}}{c^2 R_{\rm max}} + 2.43\right) M_{\rm max}$$

$$M_{\rm thres} = M_{\rm thres}(M_{\rm max}, R_{1.6}) = \left(-3.6\frac{G\, M_{\rm max}}{c^2\, R_{1.6}} + 2.38\right)\, M_{\rm max}$$

- Both better than 0.06 M_{sun}

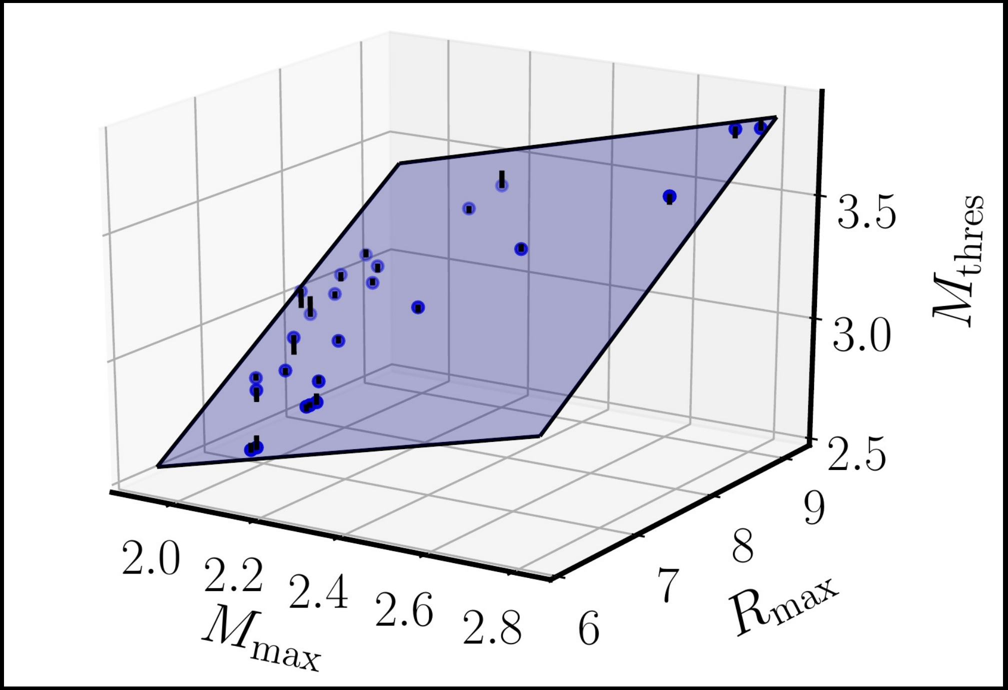

EoS constraints from GW170817*

→ lower bound on NS radii

* See also Margalit & Metzger 2017, Shibata et al. 2017, Rezzolla et al. 2018, Radice et al. 2018, Ruiz & Shapiro 2018, ... for other EoS constraints in the context of GW170817

Collapse behavior

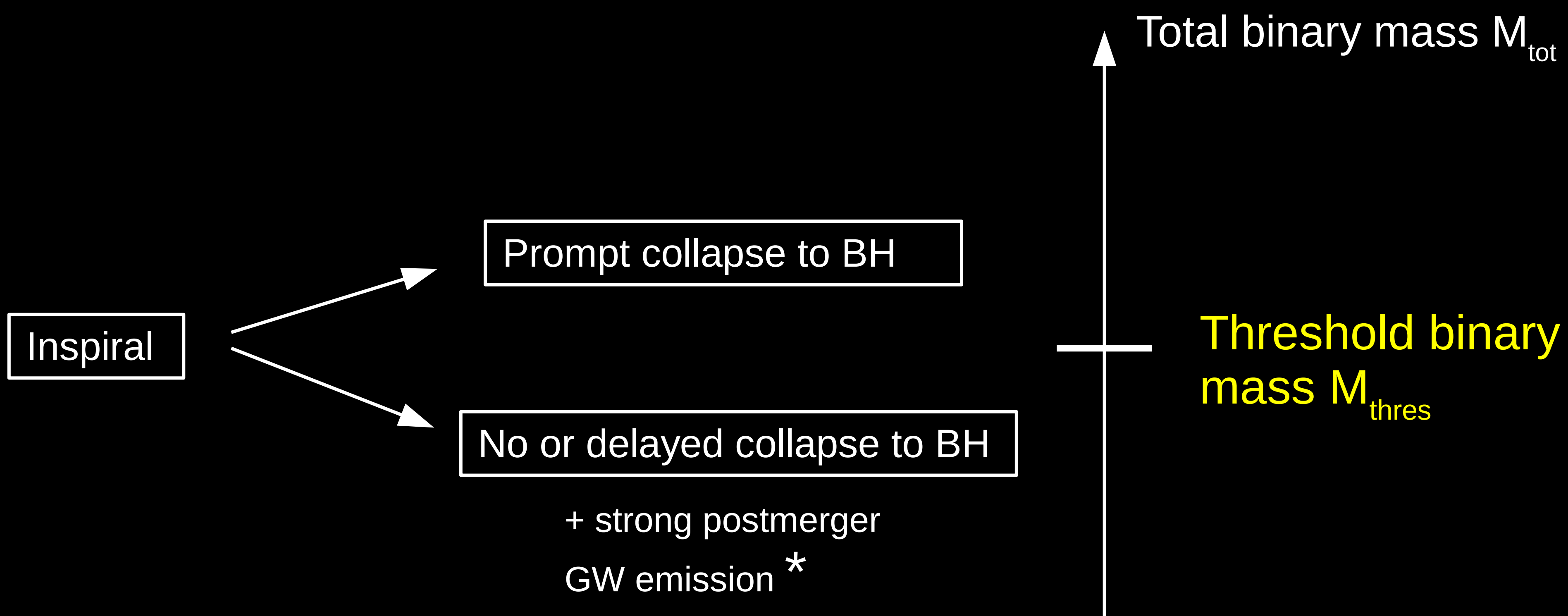

M_{thres} EoS dependent - somehow M_{max} should play a role

A simple but robust NS radius constraint from GW170817

- High ejecta mass inferred from electromagnetic transient

  → provides strong support for a delayed/no collapse in GW170817

  → even asymmetric mergers that directly collapse do not produce such massive ejecta

Reference	$m_{\rm dyn}\,[M_\odot]$	$m_{\rm w}\,[M_\odot]$
Abbott et al. (2017a)	$0.001-0.01$	–
Arcavi et al. (2017)	–	$0.02-0.025$
Cowperthwaite et al. (2017)	0.04	0.01
Chornock et al. (2017)	0.035	0.02
Evans et al. (2017)	$0.002-0.03$	$0.03-0.1$
Kasen et al. (2017)	0.04	0.025
Kasliwal et al. (2017b)	>0.02	>0.03
Nicholl et al. (2017)	0.03	–
Perego et al. (2017)	$0.005-0.01$	$10^{-5}-0.024$
Rosswog et al. (2017)	0.01	0.03
Smartt et al. (2017)	$0.03-0.05$	0.018
Tanaka et al. (2017a)	0.01	0.03
Tanvir et al. (2017)	$0.002-0.01$	0.015
Troja et al. (2017)	$0.001-0.01$	$0.015-0.03$

Compilation in Cote et al 2018

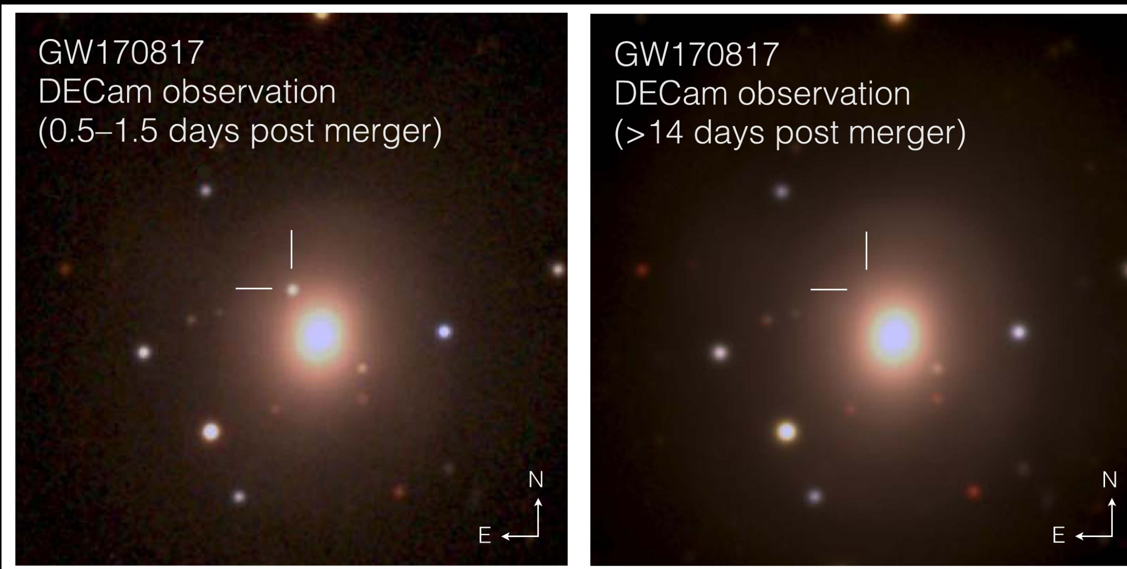

Figure 1. NGC4993 *grz* color composites ($1'.5 \times 1'.5$). Left: composite of detection images, including the discovery *z* image taken on 2017 August 18 00:05:23 UT and the g and r images taken 1 day later; the optical counterpart of GW170817 is at R.A., decl. $=197.450374, -23.381495$. Right: the same area two weeks later.

Soares-Santos et al 2017

- Ejecta masses depend on EoS and binary masses
- Note: high mass points already to soft EoS (tentatively/qualitatively)
- Prompt collapse leads to reduced ejecta mass
- Light curve depends on ejecta mass:

  → 0.02 - 0.05 M_{sun} point to delayed collapse
- Note: here only dynamical ejecta

Only dynamical ejecta

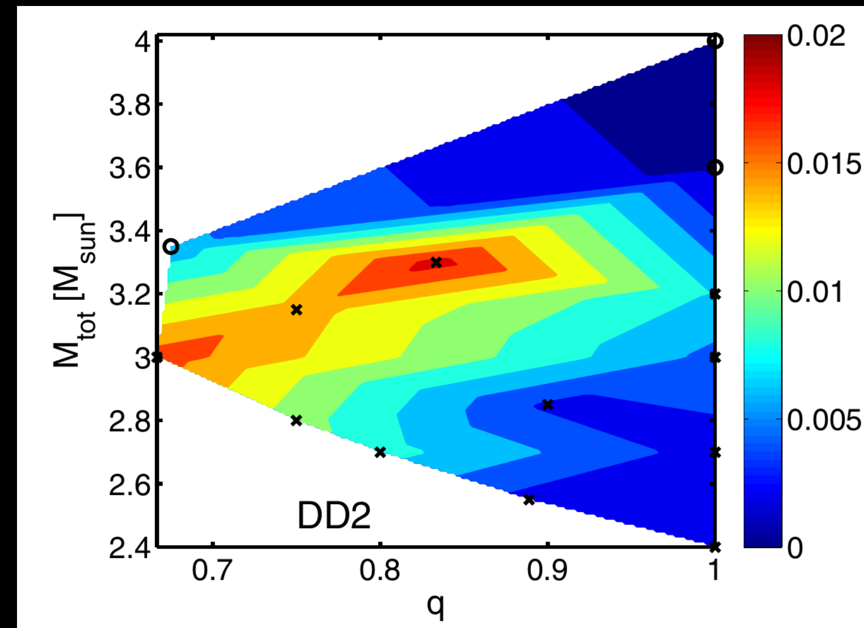

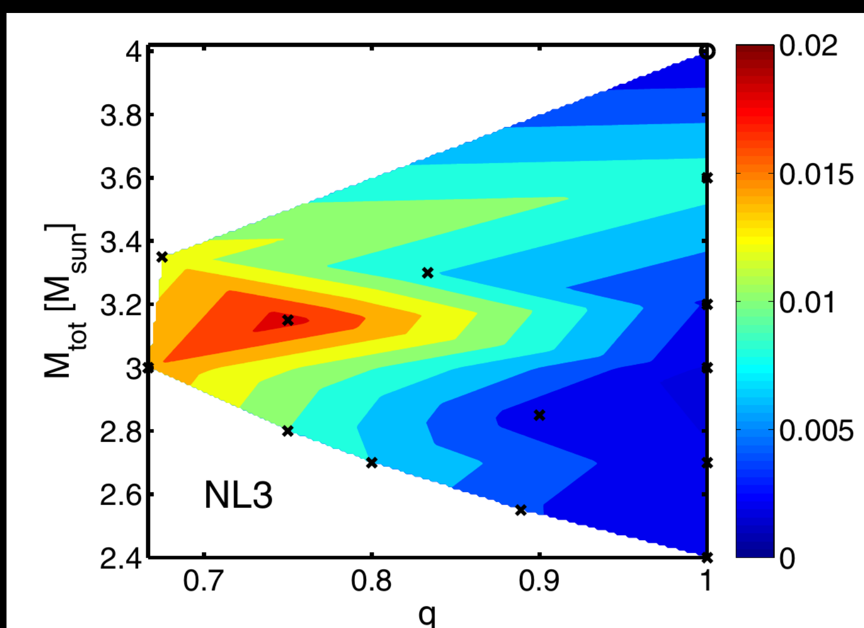

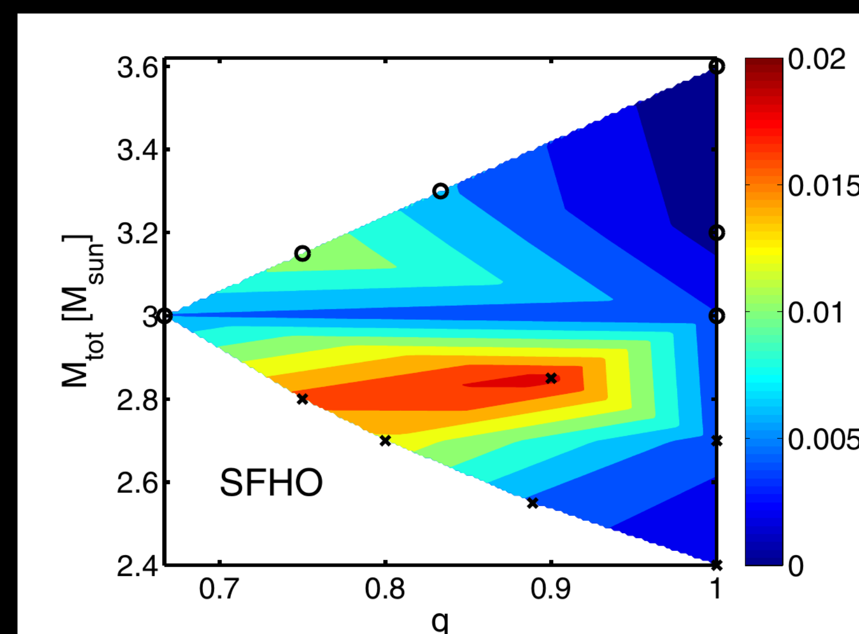

Collapse behavior

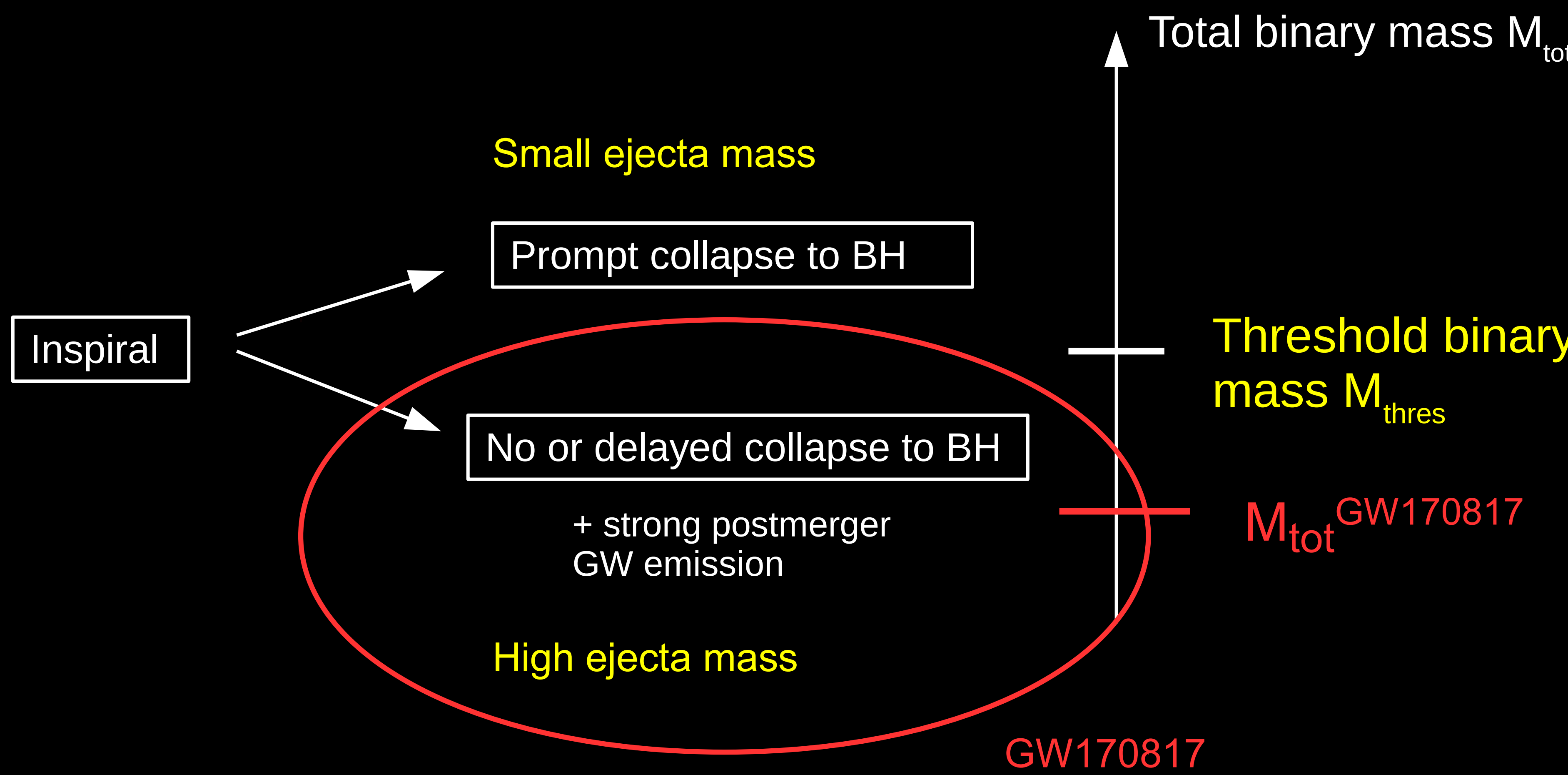

(1) If GW170817 was a delayed (/no) collapse:

$$M_{\rm thres} > M_{\rm tot}^{GW170817}$$

(2) Recall: empirical relation for threshold binary mass for prompt collapse:

$$M_{\rm thres} = \left(-3.38 \frac{G\, M_{\rm max}}{c^2\, R_{\rm max}} + 2.43\right)\, M_{\rm max} > 2.74\ M_{\odot}$$

(with $M_{\rm max}$, $R_{\rm max}$ unknown)

(3) Causality: speed of sound $v_S \leq c$ $\Rightarrow M_{\rm max} \leq \frac{1}{2.82} \frac{c^2\, R_{\rm max}}{G}$

- Putting things together:

$$M_{\rm tot}^{GW170817} \leq \left(-3.38 \frac{G\, M_{\rm max}}{c^2\, R_{\rm max}} + 2.43\right) M_{\rm max} \leq \left(-\frac{3.38}{2.82} + 2.43\right) \frac{1}{2.82} \frac{c^2\, R_{\rm max}}{G}$$

→ Lower limit on NS radius

Bauswein et al. 2017

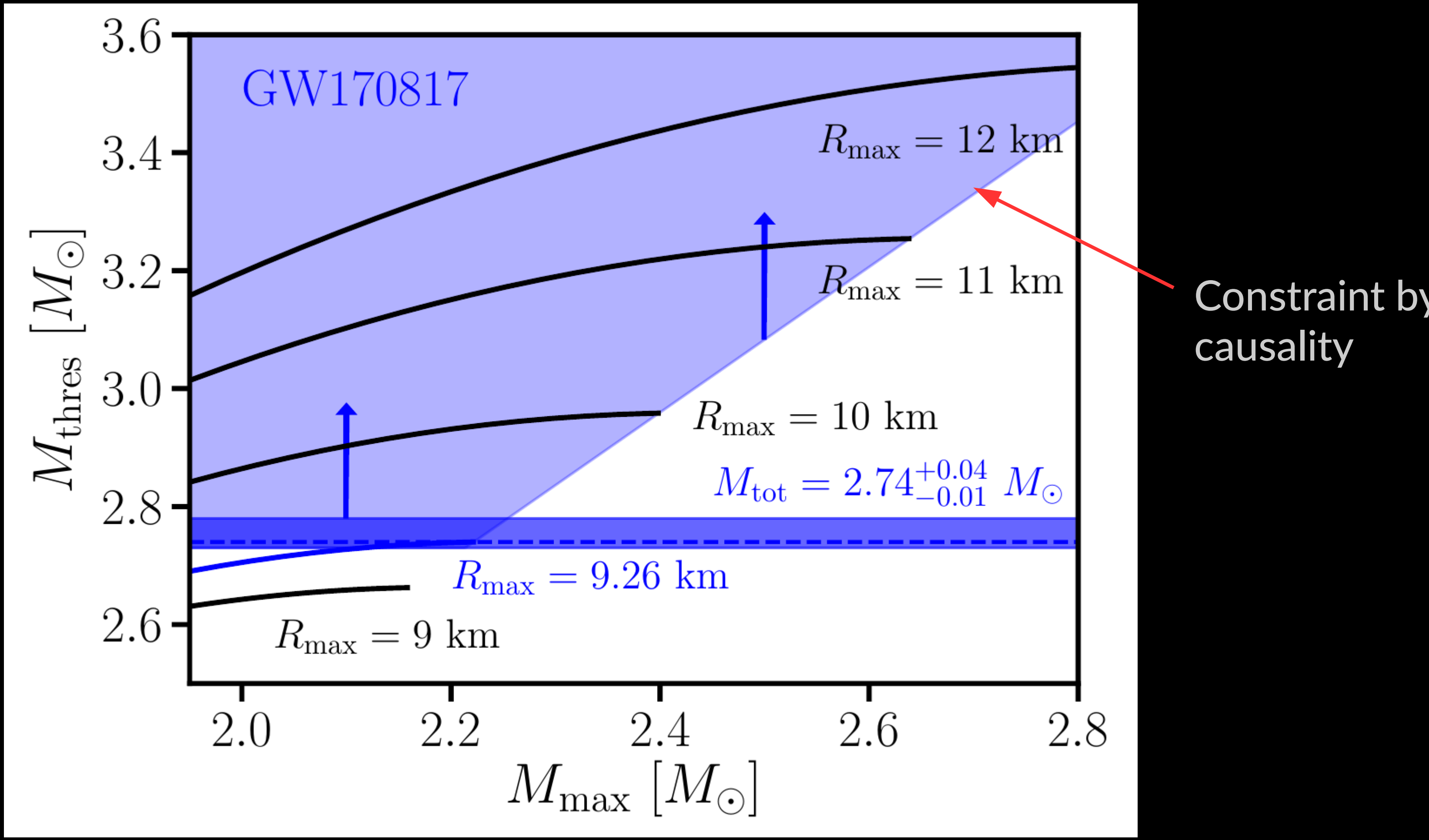

$$M_{\rm thres} = \left(-3.38\frac{GM_{\rm max}}{c^2 R_{\rm max}} + 2.43\right) M_{\rm max}$$

$$M_{\rm thres} \geq 1.2 M_{\rm max}$$

Bauswein et al. 2017

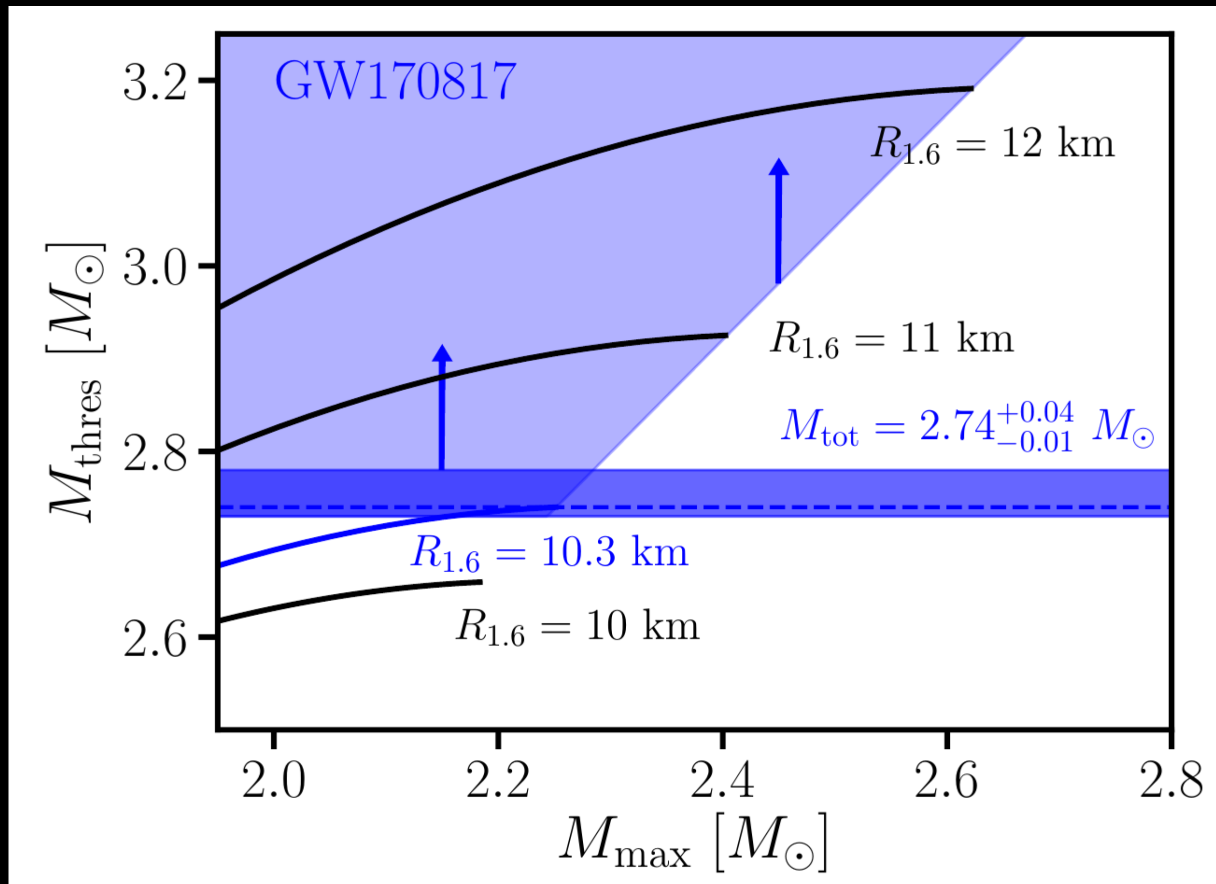

$$M_{\rm thres} = \left(-3.6\frac{G\,M_{\rm max}}{c^2\,R_{1.6}} + 2.38\right)\,M_{\rm max}$$

$$v_S = \sqrt{\frac{dP}{de}} \leq c \;\;\rightarrow\;\; M_{\rm max} \leq \kappa R_{1.6} \;\;\Rightarrow\;\; M_{\rm thres} \geq 1.2 M_{\rm max}$$

Causal limit

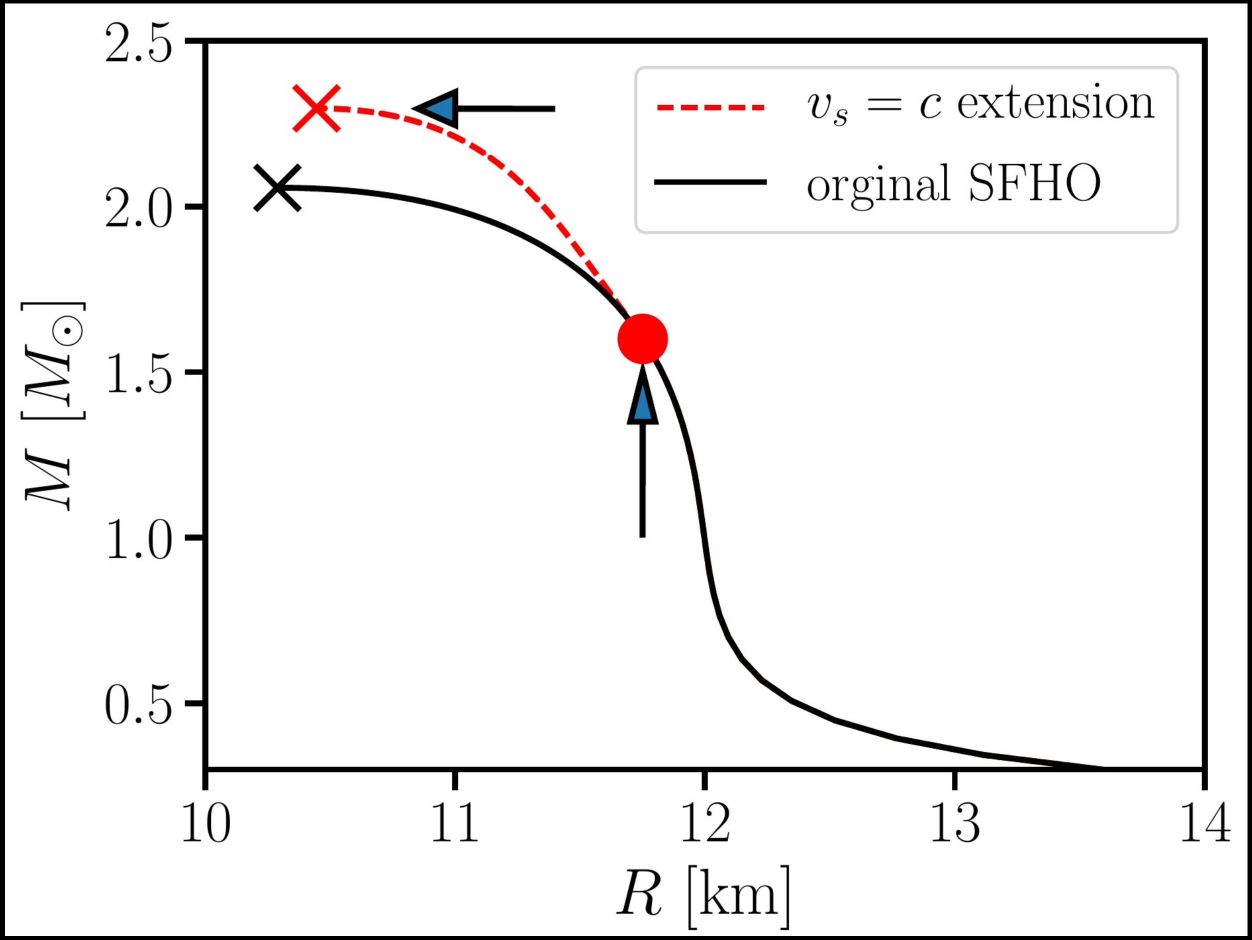

- Extend a large sample of EoS with v_s=c beyond central density of 1.6 Msun NS

$$\rightarrow \qquad v_S = \sqrt{\frac{dP}{de}} \leq c \ \rightarrow \ M_{\max} \leq \kappa R_{1.6}$$

Causality limit

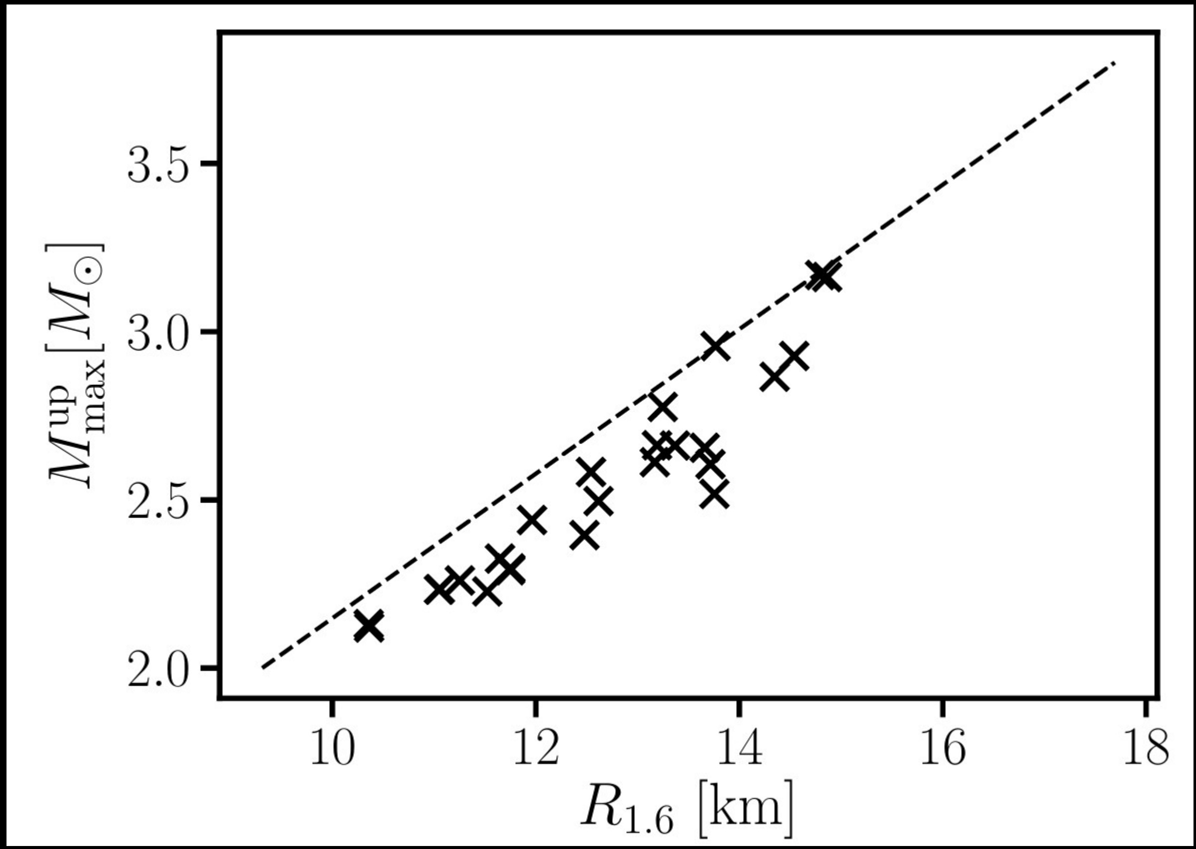

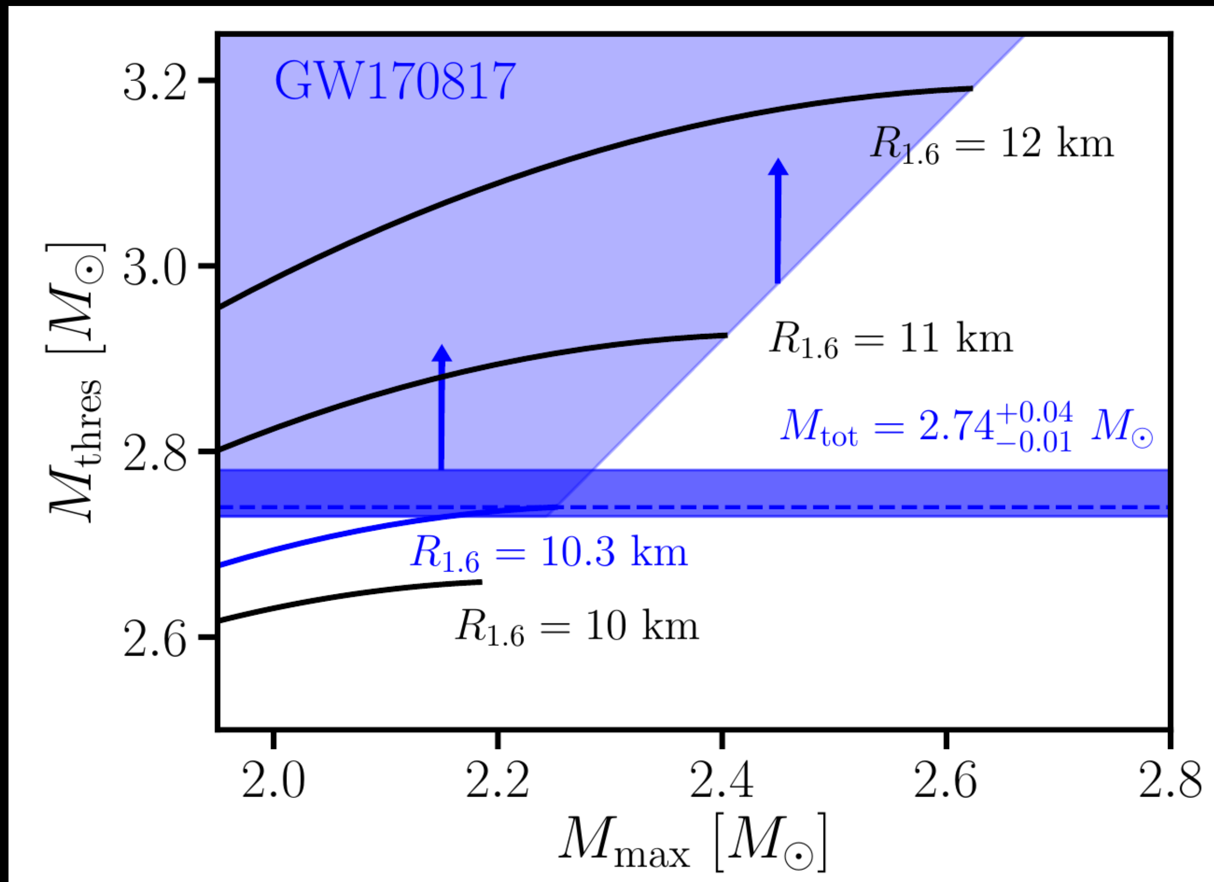

$$M_{\rm thres} = \left(-3.6 \frac{G\, M_{\rm max}}{c^2\, R_{1.6}} + 2.38\right)\, M_{\rm max}$$

$$v_S = \sqrt{\frac{dP}{de}} \leq c \;\; \rightarrow \;\; M_{\rm max} \leq \kappa R_{1.6} \;\; \Rightarrow \;\; M_{\rm thres} \geq 1.2 M_{\rm max}$$

NS radius constraint from GW170817

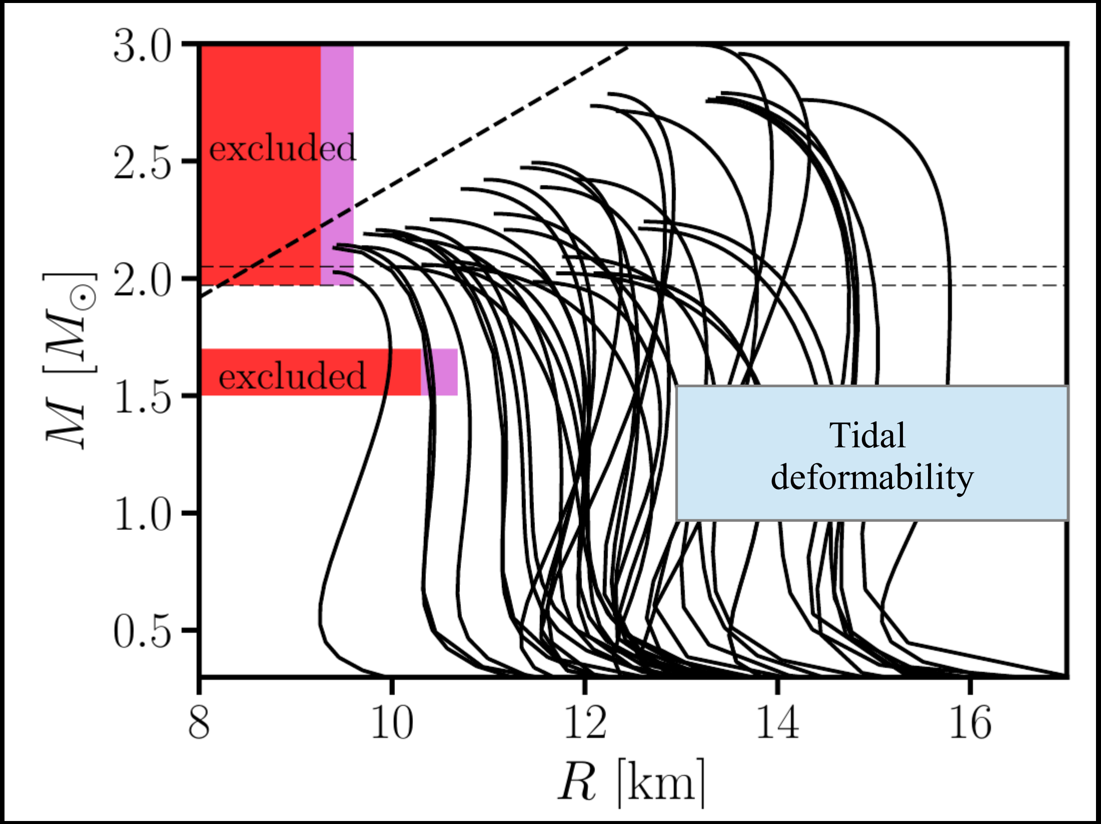

Bauswein et al. 2017

- $R_{1.6}$ > 10.7 km
- Excludes very soft nuclear matter

Radius vs. tidal deformability

Radice et al 2018

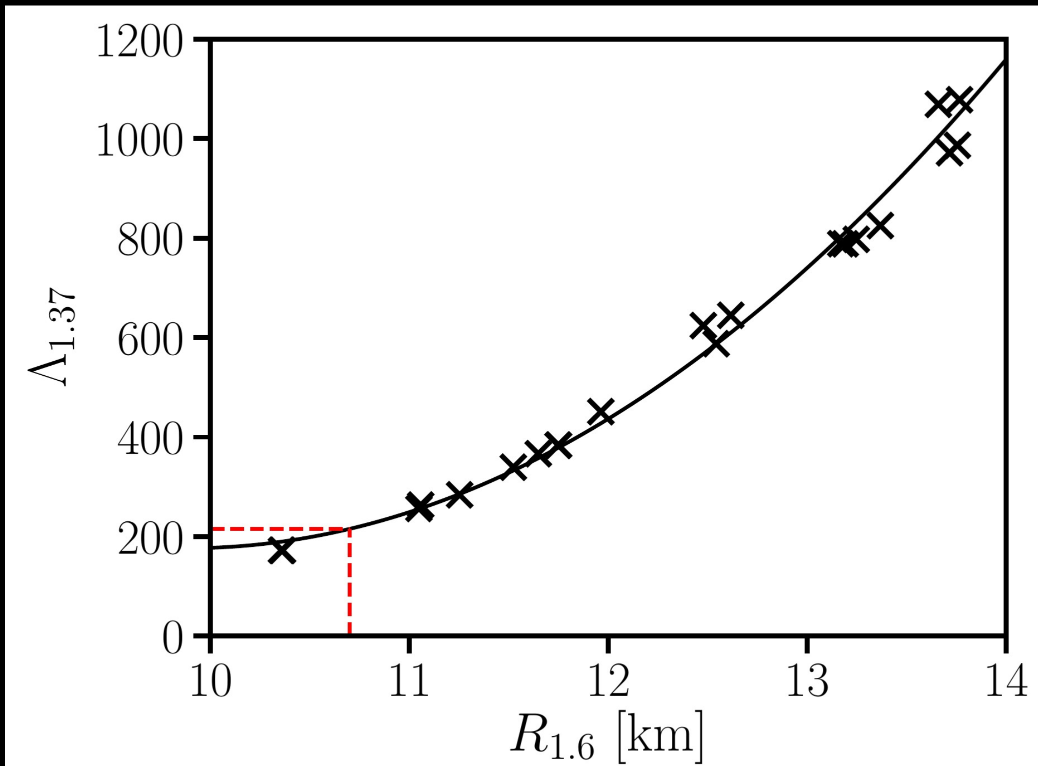

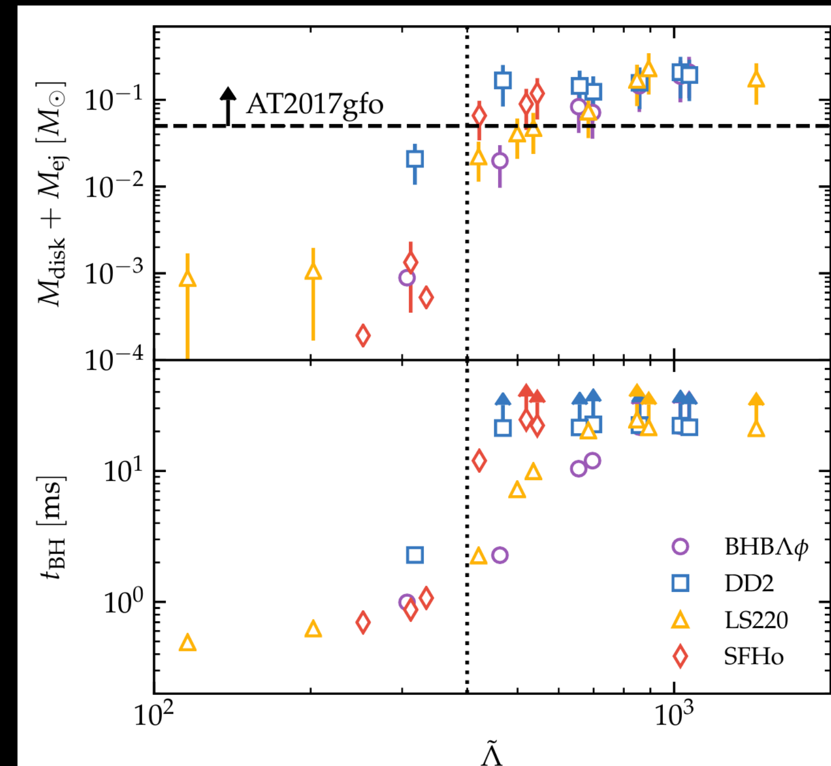

Bauswein, unpubl.

- Radius and tidal deformability scale tightly → **Lambda > 210**
- Radice et al. 2018 followed a very similar approach claiming Lambda > 400

  → only 4 EoS considered – no complete coverage existing simulation data/parameter space (see also Tews et al. 2018)

  → full EoS dependence has to be investigated via Mthres

Discussion - robustness

- Binary masses well measured with high confidence error bar
- Clearly defined working hypothesis: delayed collapse

  → testable by refined emission models

  → as more events are observed more robust distinction
- Very conservative estimate, errors can be quantified
- Empirical relation can be tested by more elaborated simulations (but unlikely that MHD or neutrinos can have strong impact on M_{thres})
- Confirmed by semi-analytic collapse model
- Low-SNR constraint !!!

Future

- Any new detection can be employed if it allows distinction between prompt/delayed collapse
- With more events in the future our comprehension of em counterparts will grow → more robust discrimination of prompt/delayed collapse events
- Low-SNR detections sufficient !!! → that's the potential for the future

  → we don't need louder events, but more

  → complimentary to existing ideas for EoS constraints

Future detections (hypothetical discussion)

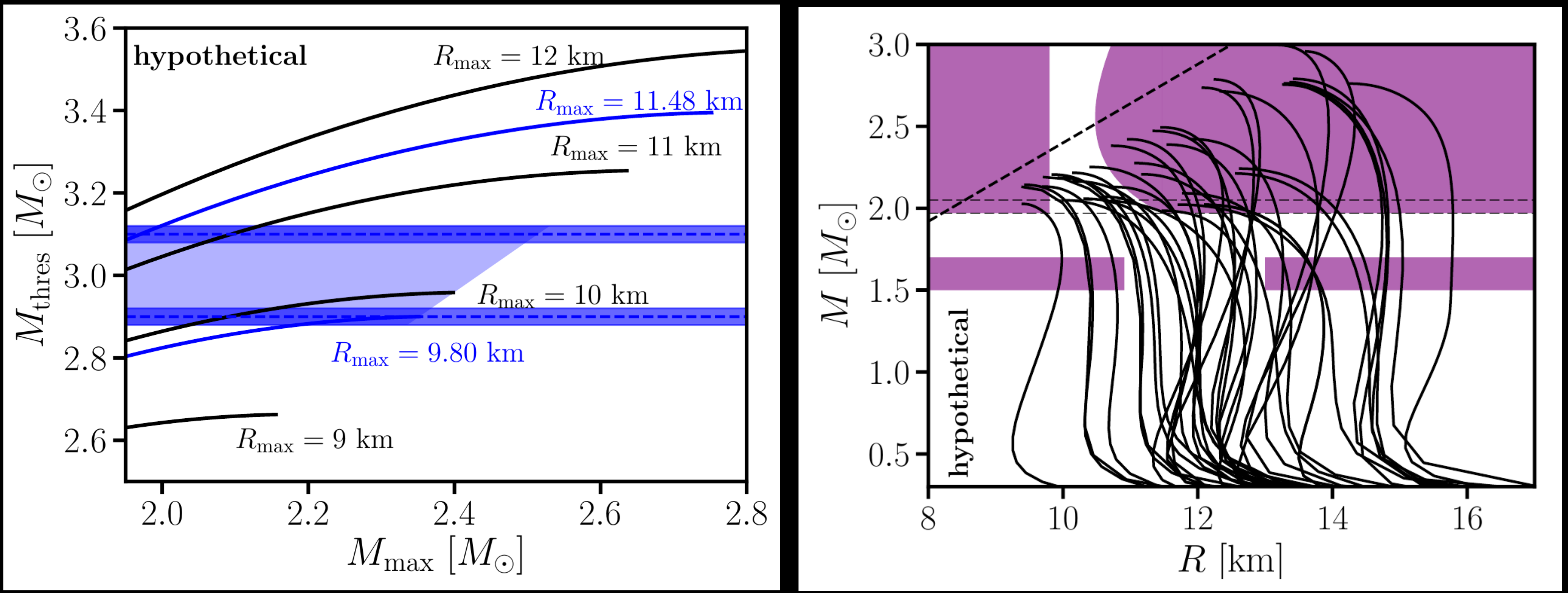

→ as more events are observed, bands converge to true M_{thres}

→ prompt collapse constrains M_{max} from above

Bauswein et al. 2017

Future plans

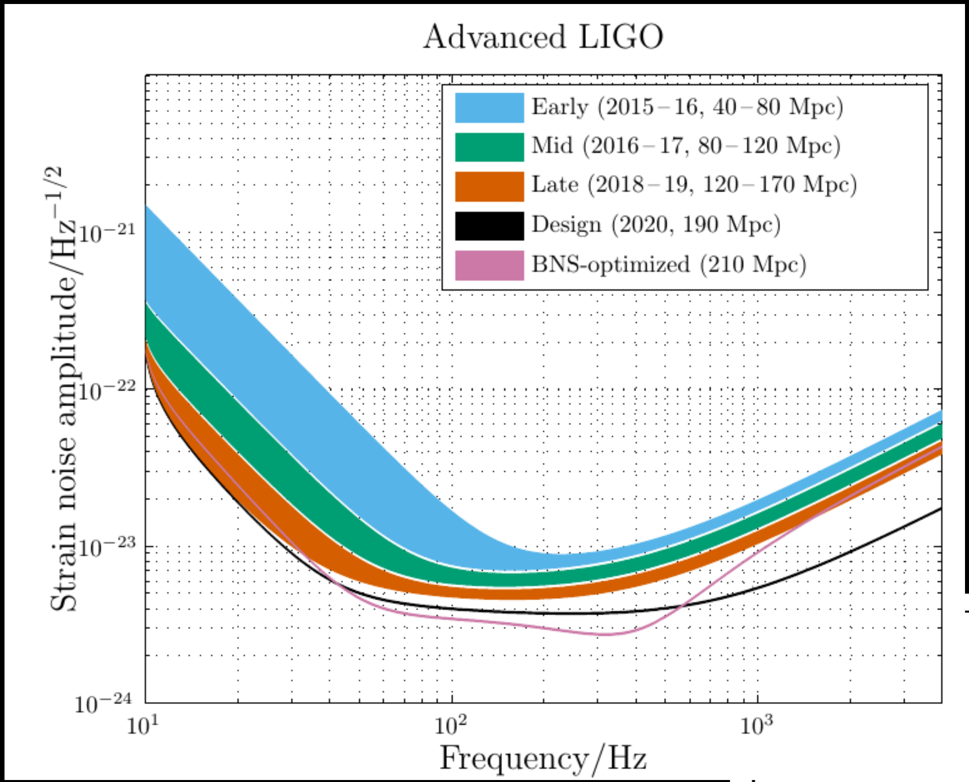

Abbott et al. 2017

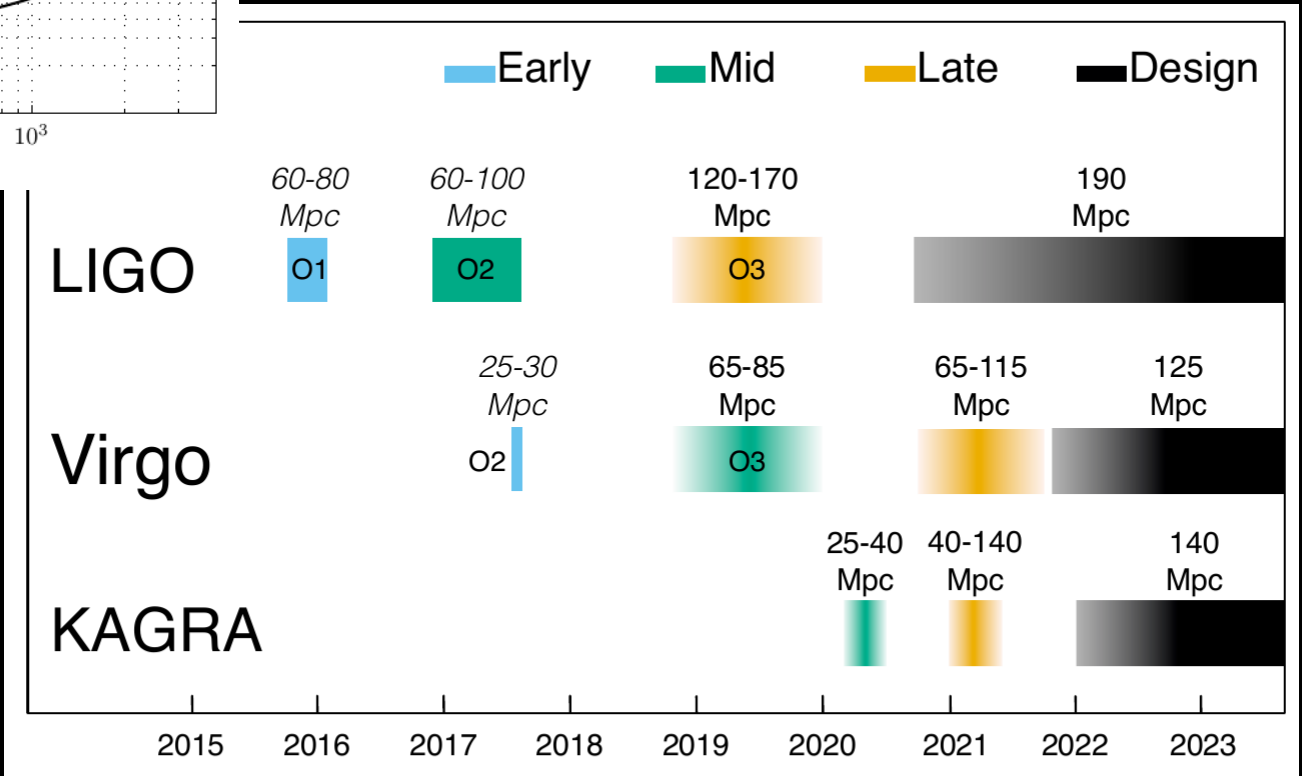

M_{max} from GW170817

- Arguments: no prompt collapse; no long-lasting pulsar spin-down (too less energy deposition)
- If GW170817 did not form a supramassive NS (rigidly rotating > M_{max})

→ M_{max} < ~2.2-2.4 M_{sun} (relying on some assumption)

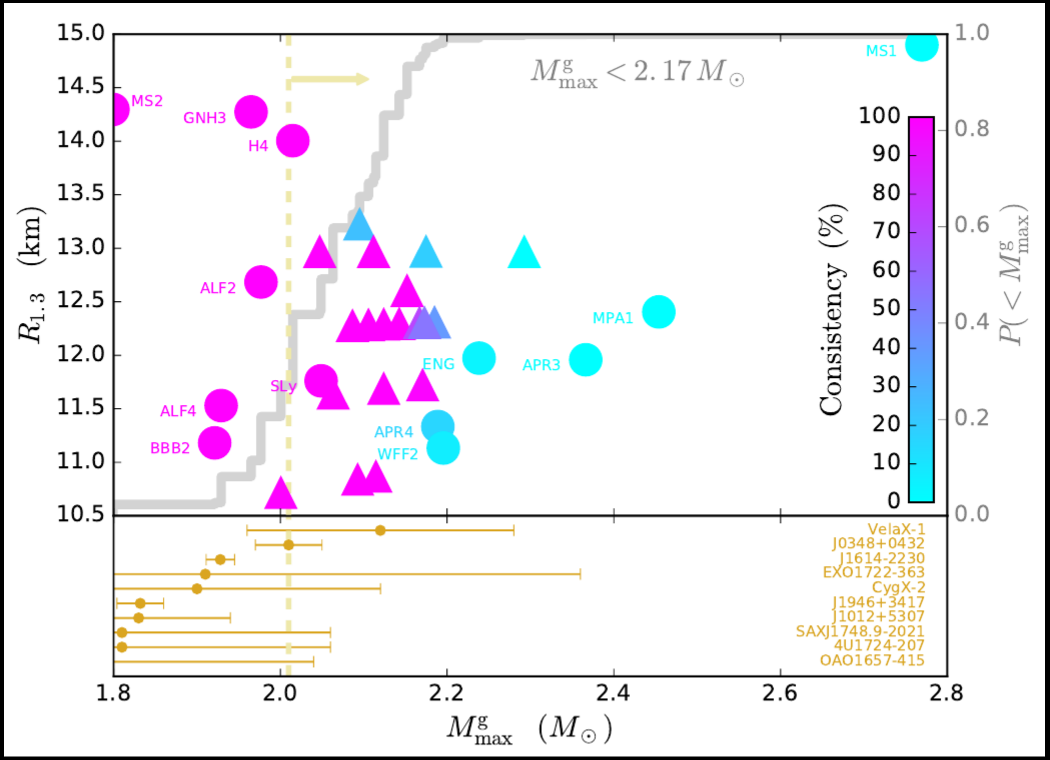

Margalit & Metzger 2017

Future: Maximum mass

- Empirical relation

$$M_{\rm thres} = \left(-3.6\frac{G\,M_{\rm max}}{c^2\,R_{1.6}} + 2.38\right)\,M_{\rm max}$$

- Sooner or later we'll know $R_{1.6}$ (e.g. from postmerger) and M_{thres} (from several events – through presense/absence of postmerger GW emission or em counterpart)

  => direct inversion to get precise estimate of M_{max}

  (see also current estimates e.g. by Margalit & Metzger, Rezzolla et al, Ruiz & Shapiro, Shibata et al., ...)

Postmerger GW emission*

(dominant frequency of postmerger phase)

→ determine properties of EoS/NSs

→ postmerger GW spectrum reveals dynamics

* not detected for GW170817 – expected for current sensitivity and d=40 Mpc (Abbott et al. 2017)

Postmerger

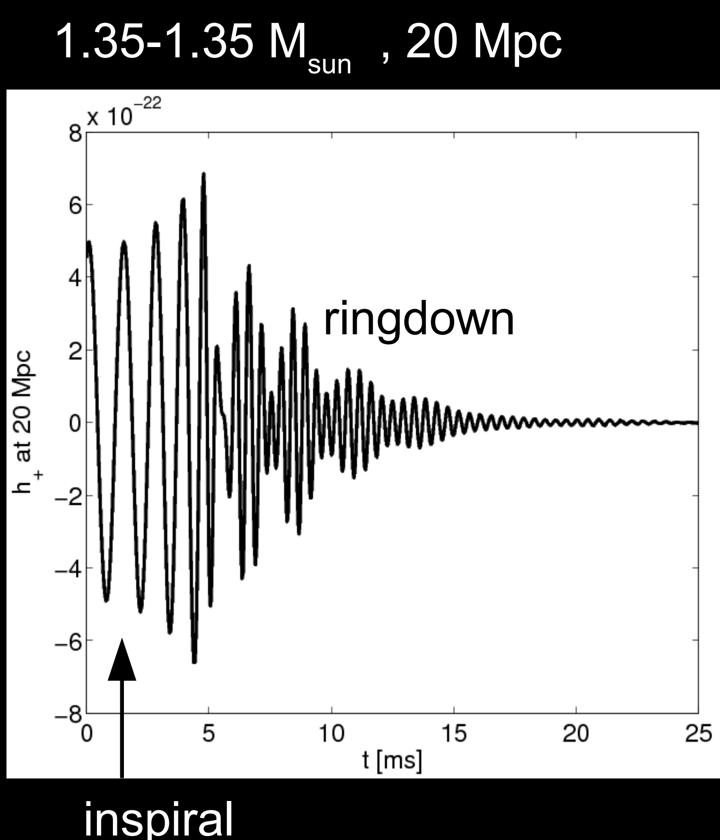

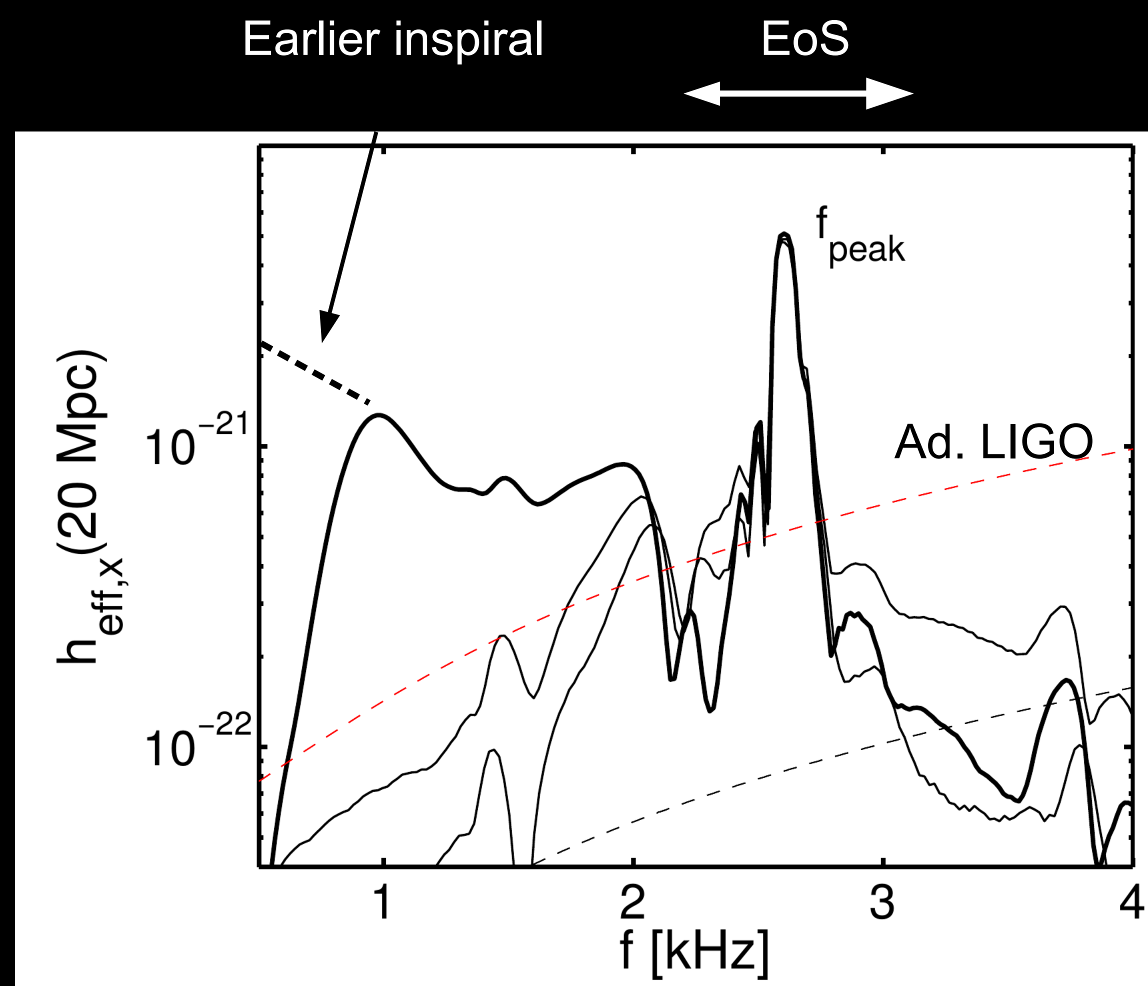

Dominant postmerger oscillation frequency f_{peak}

Very characteristic (robust feature in all models)

Gravitational waves – EoS survey

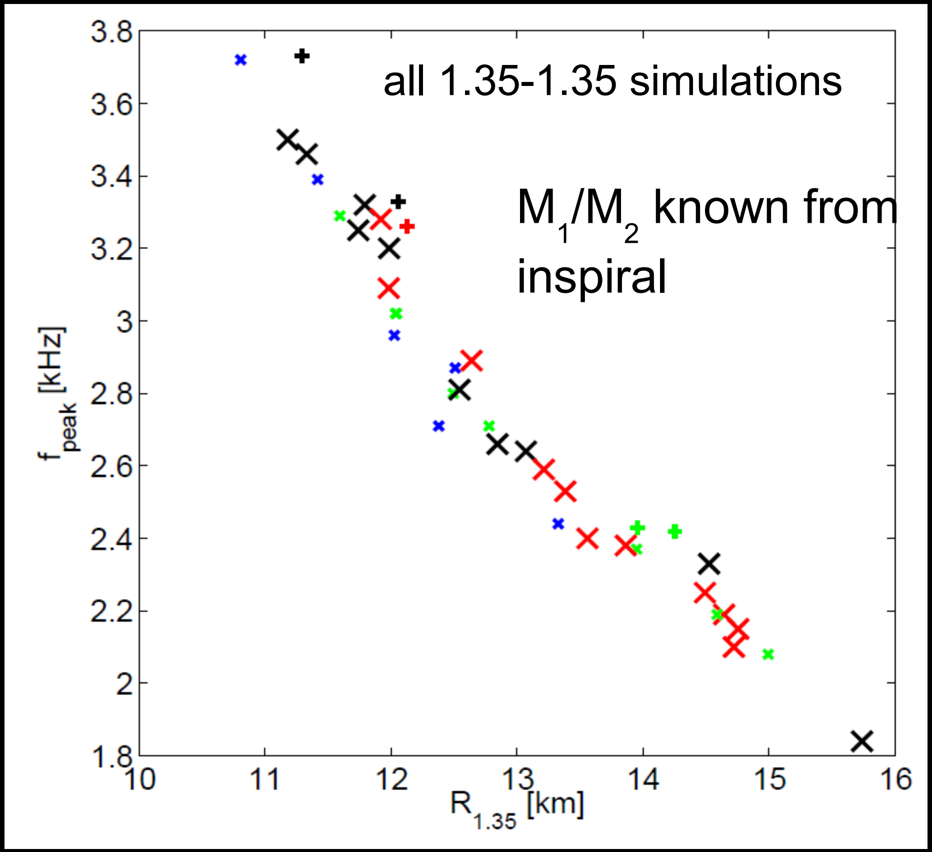

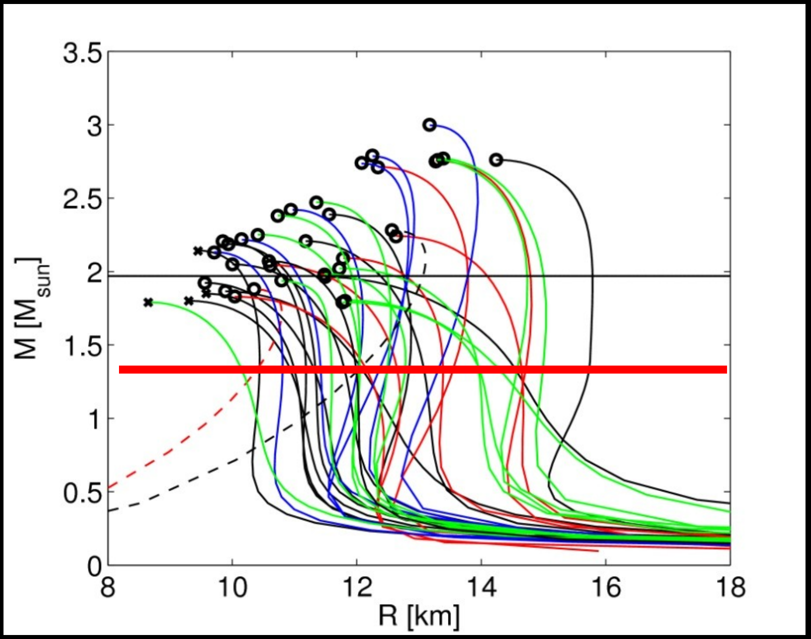

characterize EoS by radius of nonrotating NS with 1.35 M_{sun}

Bauswein et al. 2012

Pure TOV/EoS property => Radius measurement via f_{peak}

Here only 1.35-1.35 Msun mergers (binary masses measurable) – similar relations exist for other fixed binary setups !!!

~ 40 different NS EoSs

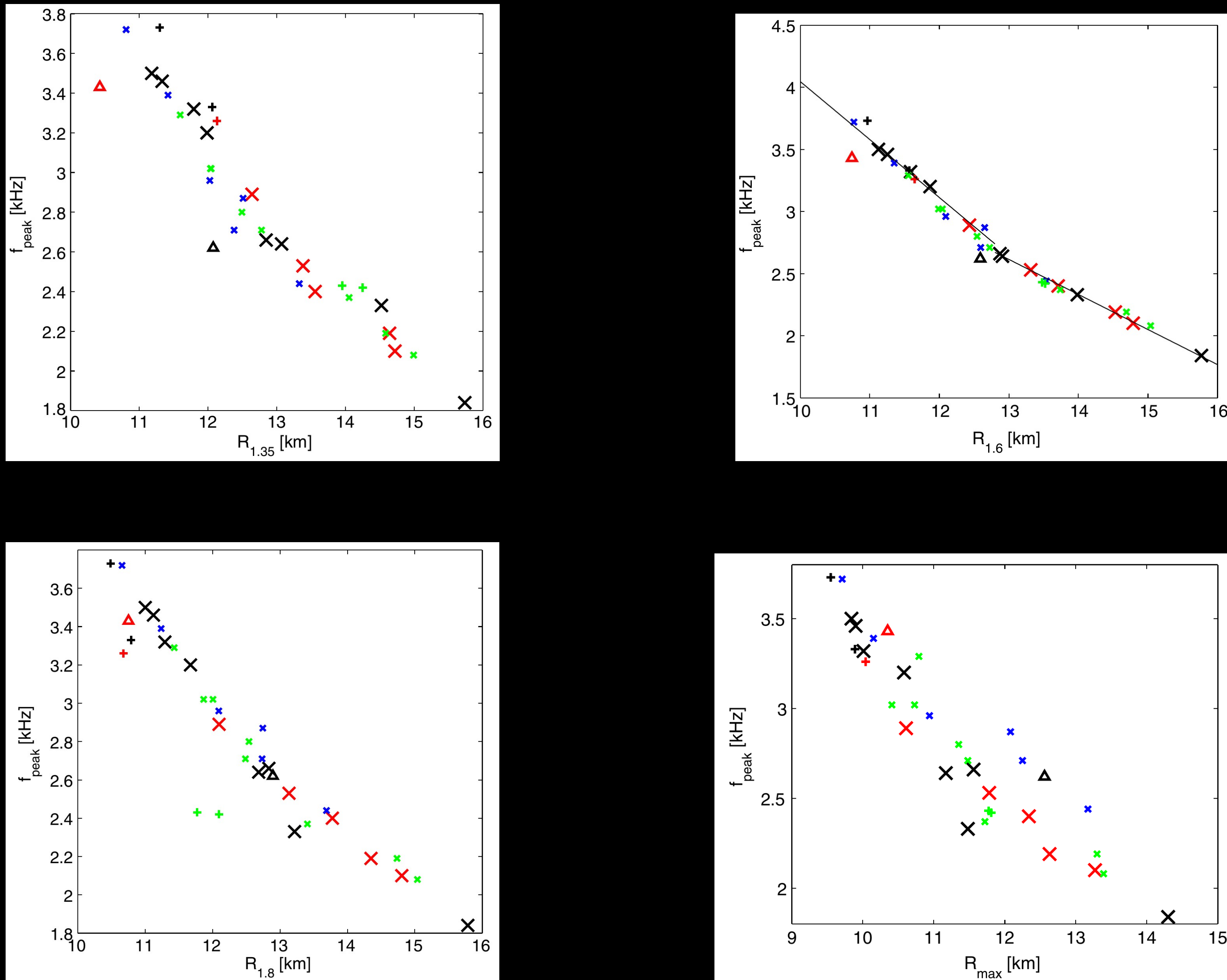

Bauswein et al. 2012

Assess quality of empirical relation relation – only infinity norm meaningful !!!

→ as many EoS models as possible !!!

Gravitational waves – EoS survey

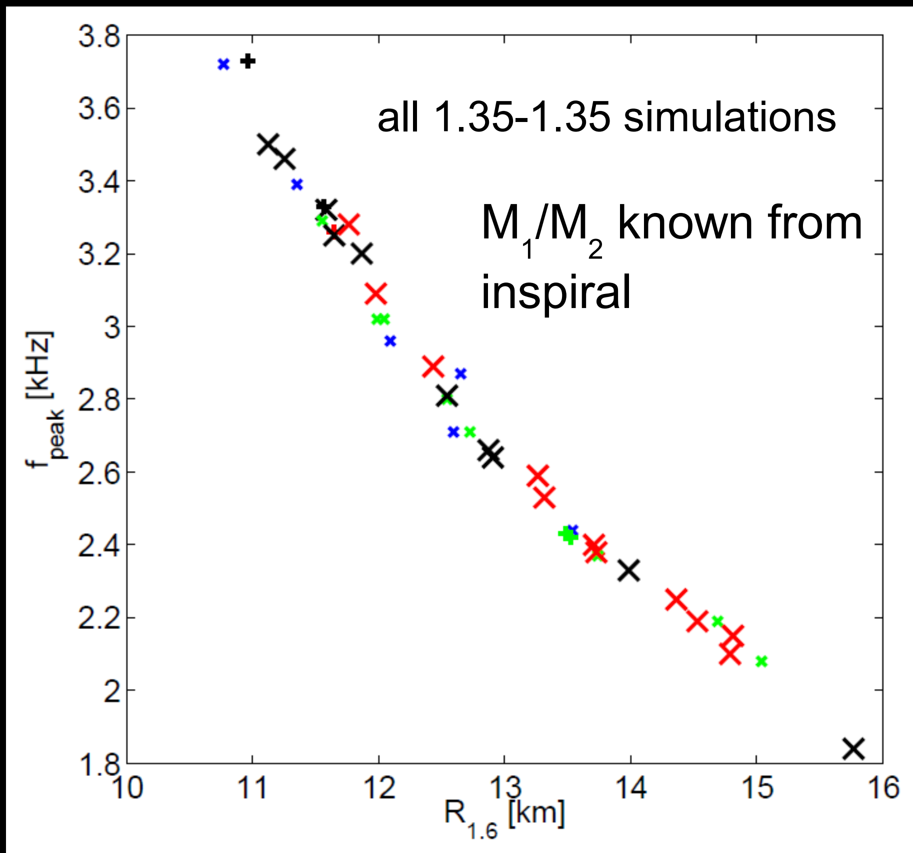

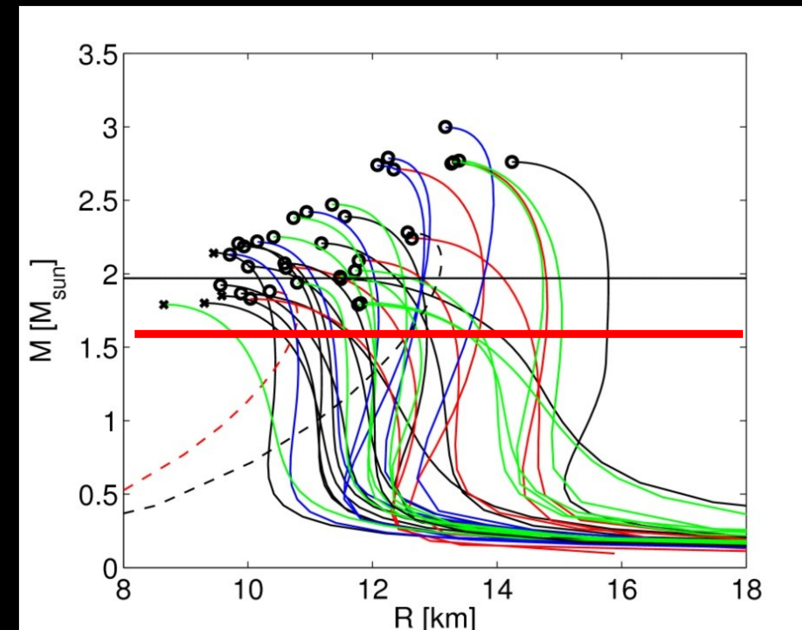

characterize EoS by radius of nonrotating NS with 1.6 M_{sun}

Bauswein et al. 2012

Pure TOV/EoS property => Radius measurement via f_{peak}

Smaller scatter in empirical relation (< 200 m) → smaller error in radius measurement

Note: R of 1.6 M_{sun} NS scales with f_{peak} from 1.35-1.35 M_{sun} mergers (density regimes comparable)

Binary mass variations

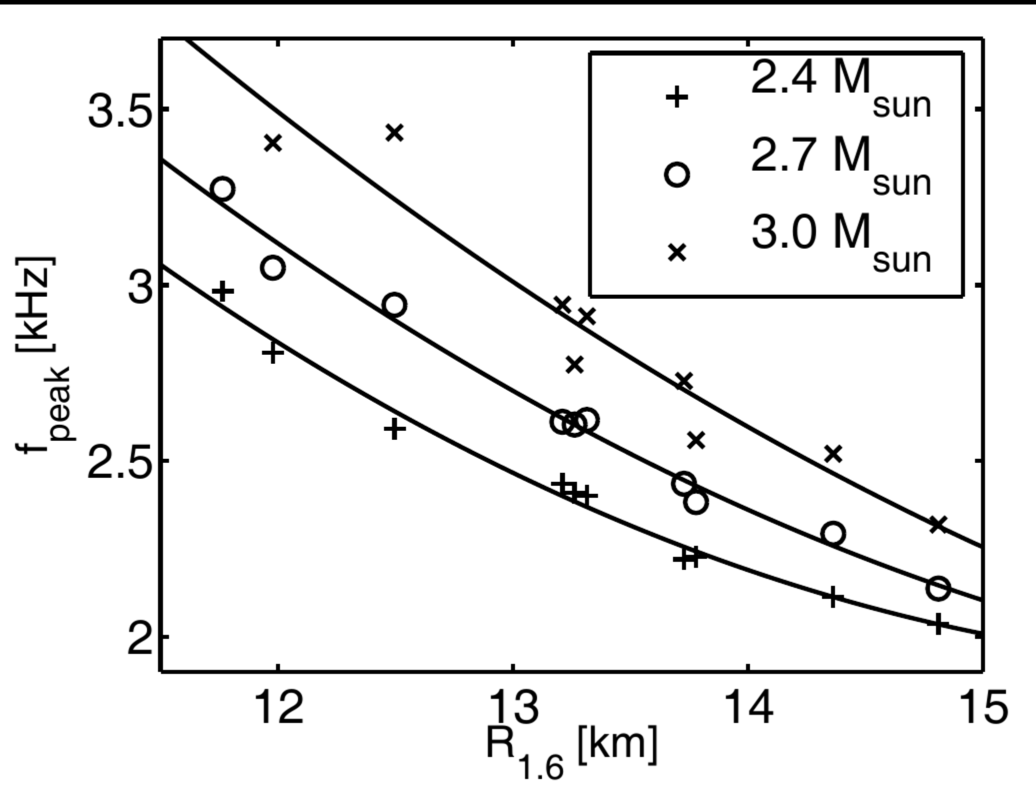

Different total binary masses (symmetric)

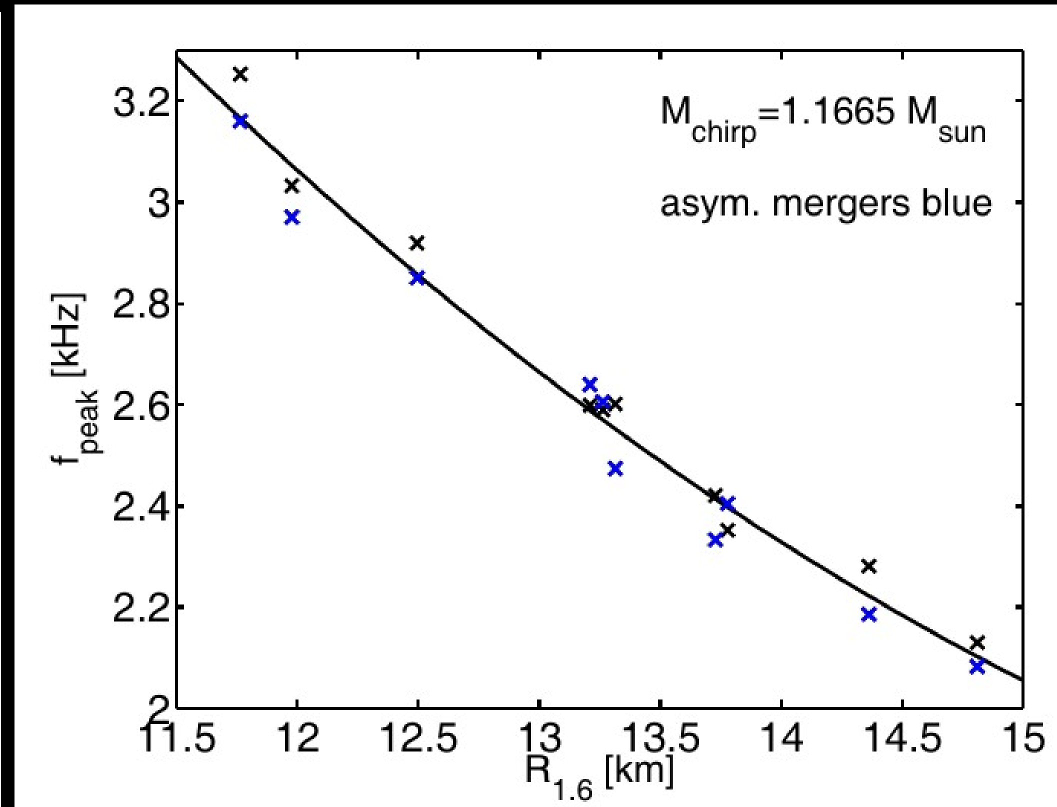

Fixed chirp mass (asymmertic 1.2-1.5 M_{sun} binaries and symmetric 1.34-1.34 M_{sun} binaries)

Data analysis: see e.g. Clark et al. 2016 (PCA), Clark et al. 2014 (burst search), Chatziioannou et al 2017

→ f_{peak} precisely measurable !!!

Bauswein et al. 2012, 2016

Strategy for radius measurements

- Measure binary masses from inspiral
- Construct f_{peak} – R relation for this fixed binary masses and (optimally) chosen R
- Measure f_{peak} from postmerger GW signal
- Obtain radius by inverting f_{peak} – R relation
- (possibly restrict to fixed mass ratios if mergers with high asymmetry are measured)

- Final error of radius measurement:

  - accuracy of f_{peak} measurement (see Clark et al. 2014, Clark et al. 2016)

  - maximum scatter in f-R relation (important to consider very large sample of EoSs)

  - systematic error in f-R relation

Data analysis

- Principal Component analysis

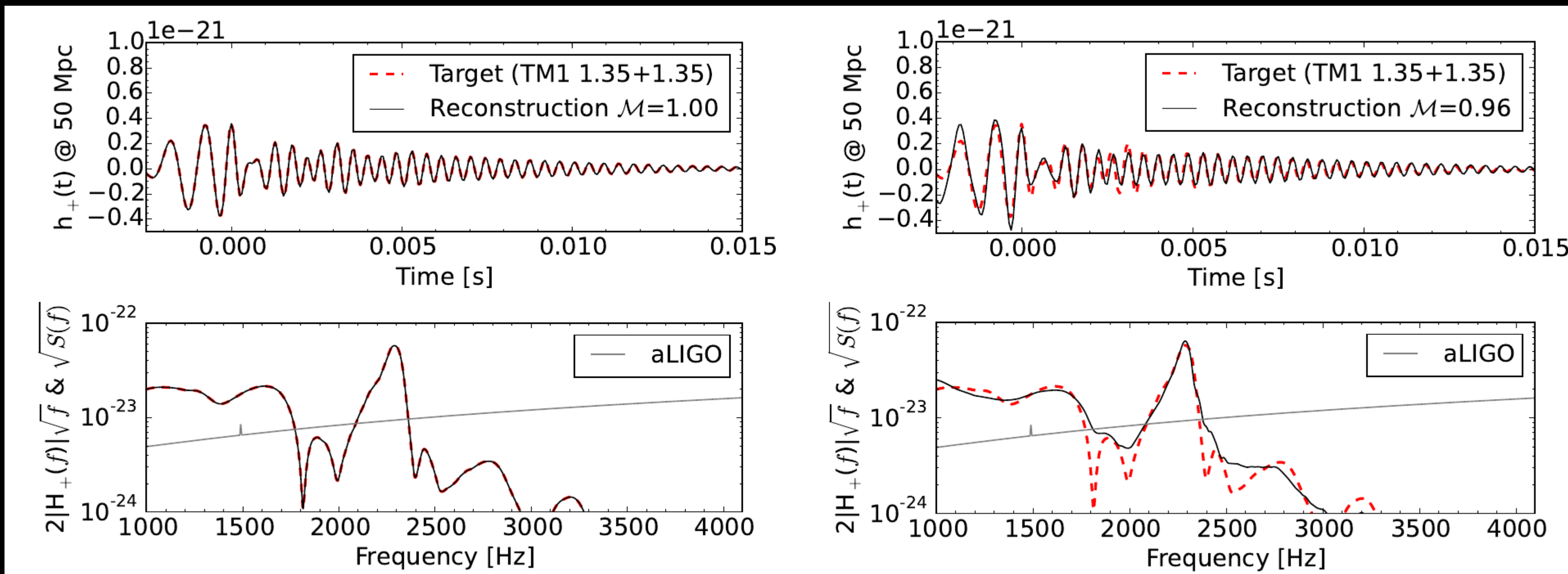

Excluding recovered waveform from catalogue

Clark et al. 2016, see also Clark et al 2014, Chatziioannou et al 2017, Bose et al. 2018

Instrument	$\mathrm{SNR}_{\mathrm{full}}$	D_{hor} [Mpc]	$\dot{N}_{\mathrm{det}}$ [year^{-1}]
aLIGO	$2.99^{3.86}_{2.37}$	$29.89^{38.57}_{23.76}$	$0.01^{0.03}_{0.01}$
A+	$7.89^{10.16}_{6.25}$	$78.89^{101.67}_{62.52}$	$0.13^{0.20}_{0.10}$
LV	$14.06^{18.13}_{11.16}$	$140.56^{181.29}_{111.60}$	$0.41^{0.88}_{0.21}$
ET-D	$26.65^{34.28}_{20.81}$	$266.52^{342.80}_{208.06}$	$2.81^{5.98}_{1.33}$
CE	$41.50^{53.52}_{32.99}$	$414.62^{535.221}_{329.88}$	$10.59^{22.78}_{5.33}$

Outdated!!!

→ possible at Ad. LIGO's design sensitivity !

Model-agnostic data analysis

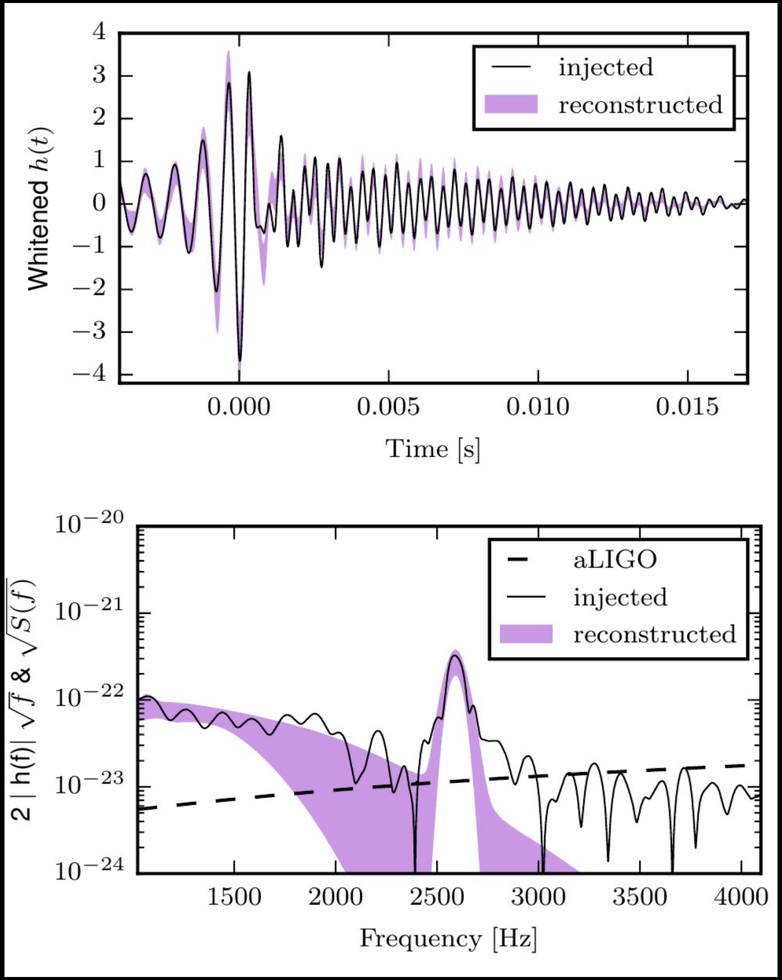

Based on wavelets

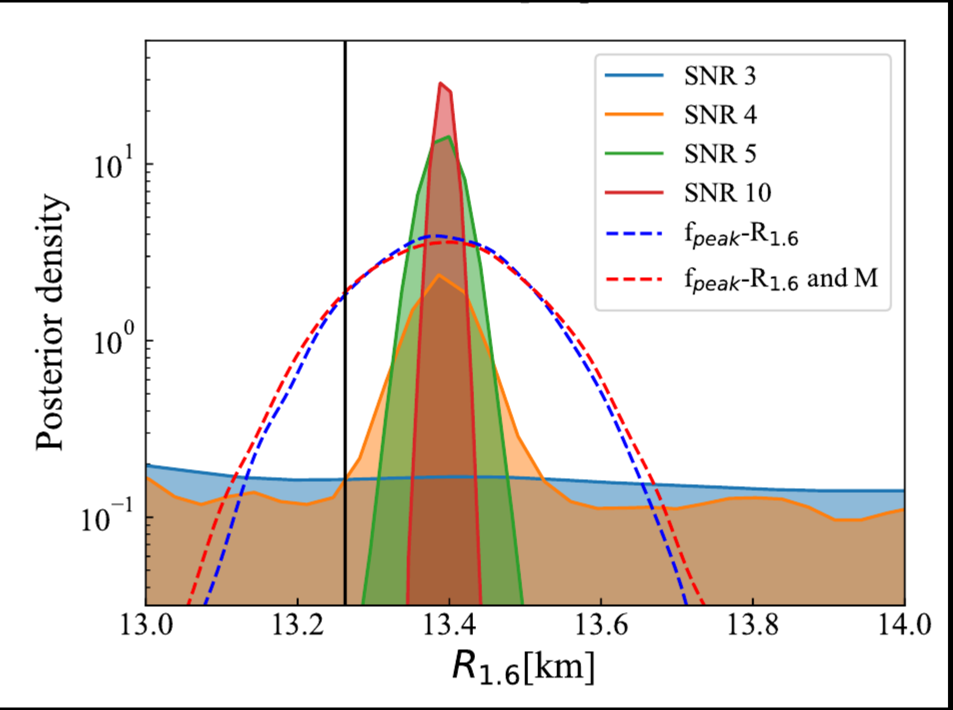

Chatziioannou et al. (2017)

Inferring the pressure at fixed density

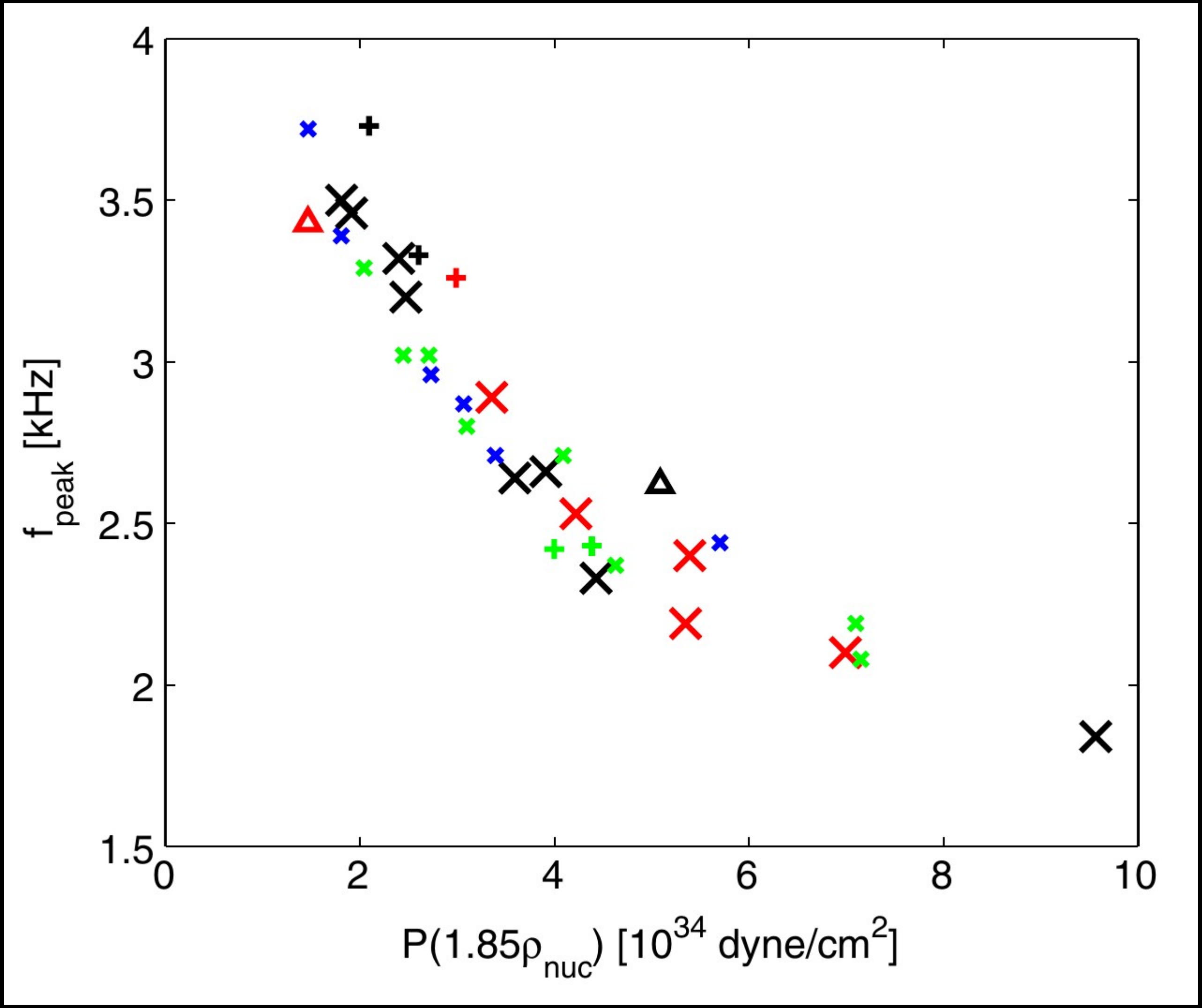

1.35-1.35 Msun

Bauswein et al. 2012

Observable signature of (QCD) phase transition

Phase diagram of matter

GSI/FAIR

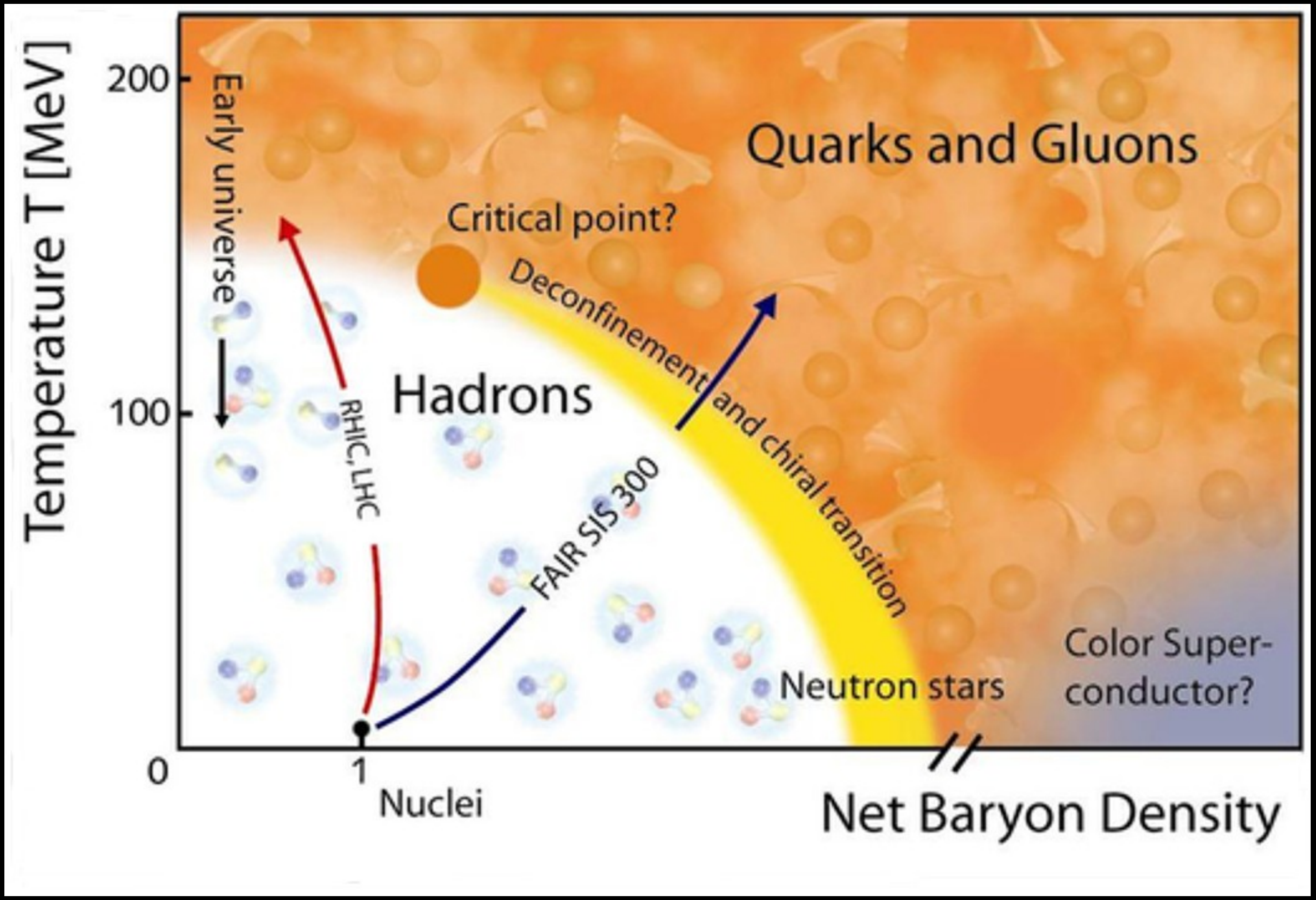

Does the phase transition to quark-gluon plasma occur (already) in neutron stars or only at higher densities?

EoS with 1st-order phase transition to quark matter

Bauswein et al. 2018

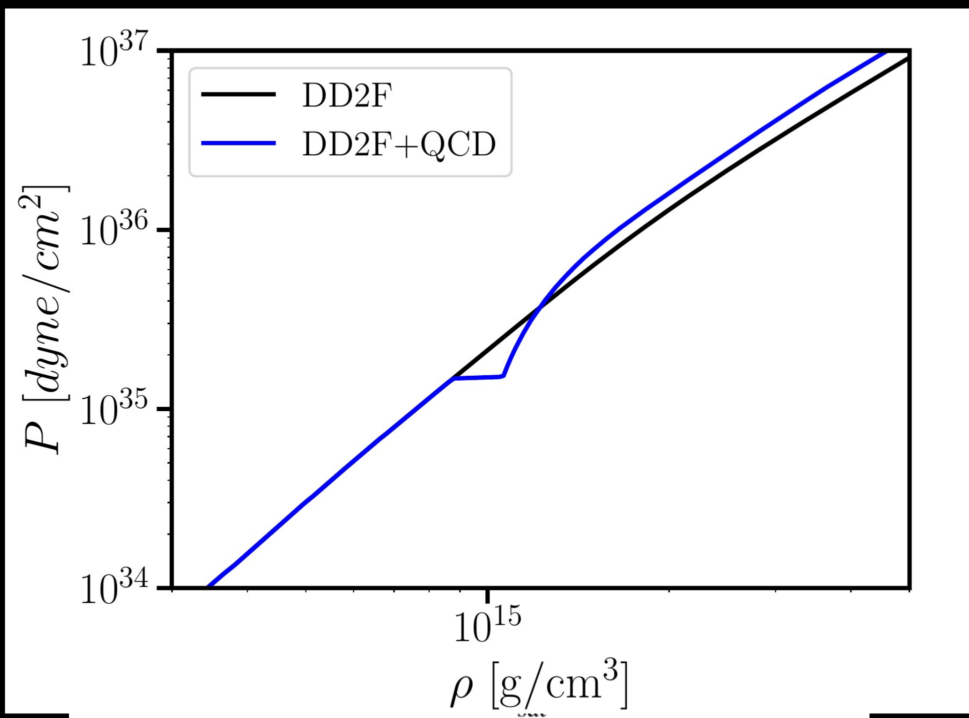

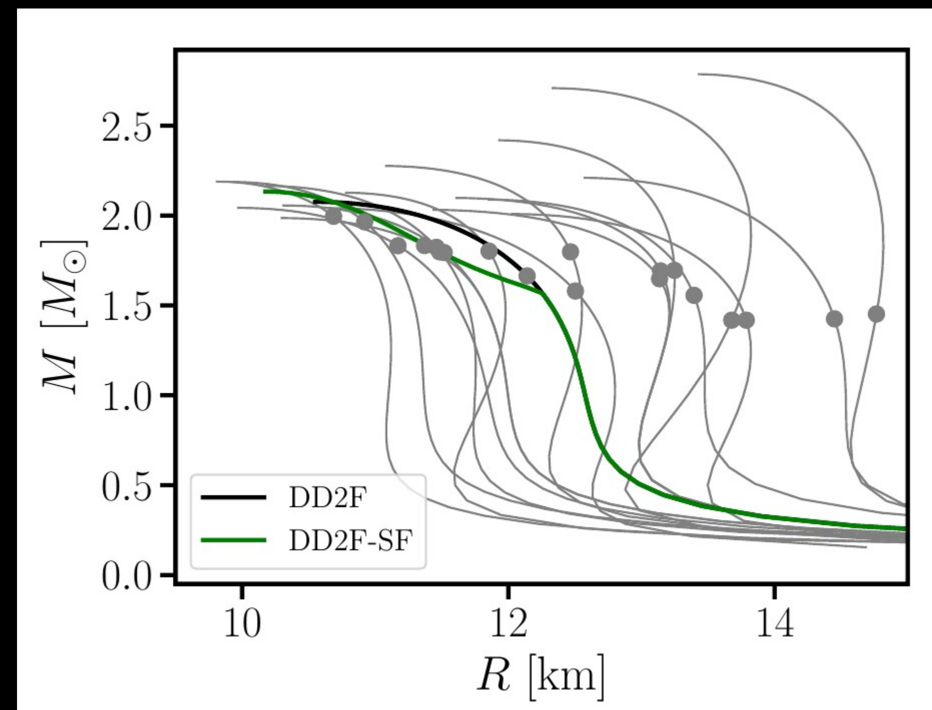

- EoS from Fischer et al. 2018 – as one example for an EoS with a strong 1st-order phase transition to deconfined quarks

Merger simulations

- GW spectrum 1.35-1.35 Msun

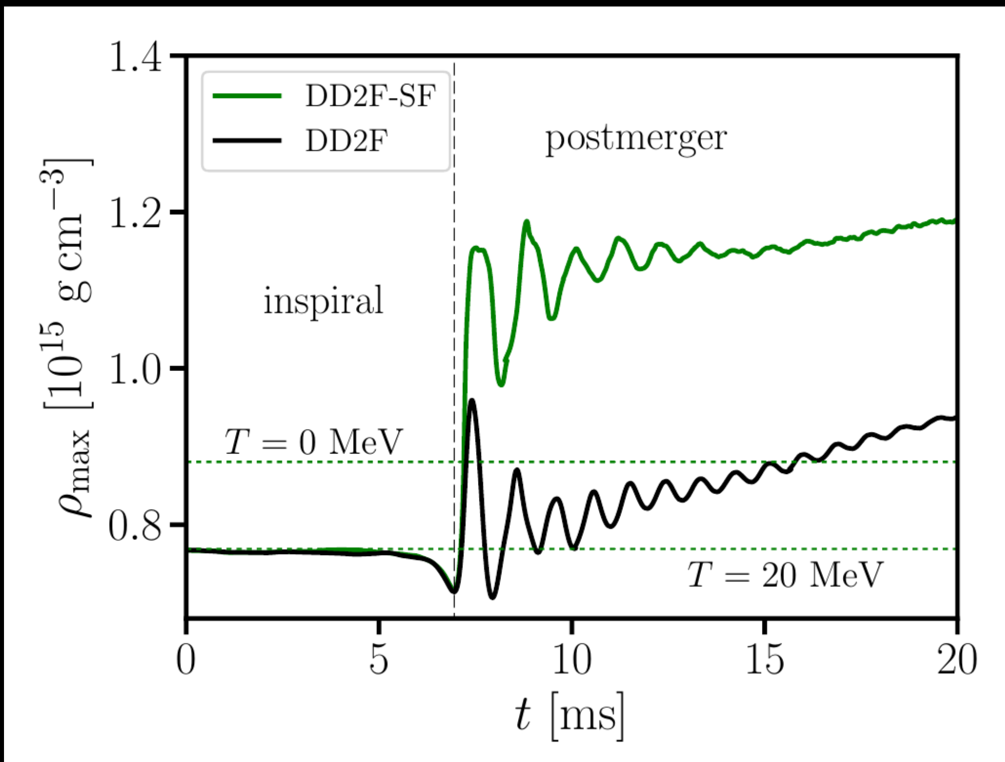

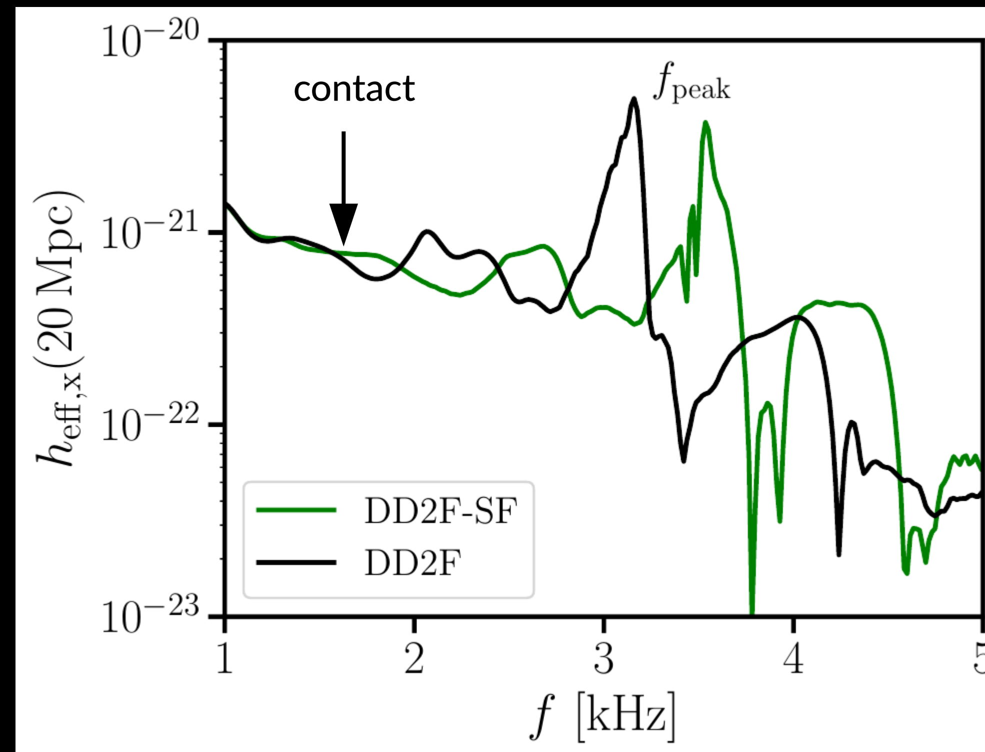

Bauswein et al. 2018

But: a high frequency on its own may not yet be characteristic for a phase transition

→ unambiguous signature

(→ show that all purely baryonic EoS behave differently)

Signature of 1st order phase transition

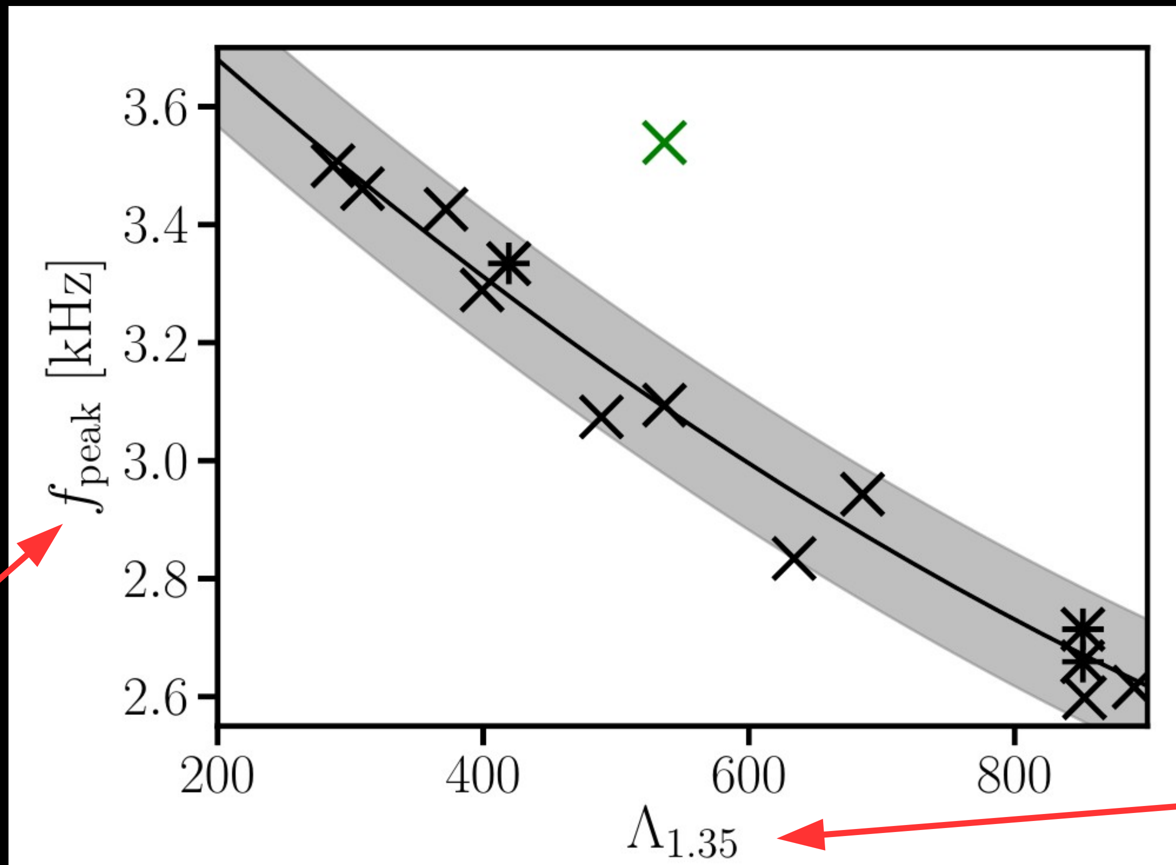

from postmerger

from the inspiral

Bauswein et al. 2018

- Tidal deformability measurable from inspiral to within 100-200 (Adv. Ligo design)
- Postmerger frequency measurable to within a few 10 Hz @ a few 10 Mpc (either Adv. Ligo or upgrade)
- Important: “all” purely hadronic EoSs (including hyperonic EoS) follow fpeak-Lambda relation → deviation characteristic for strong 1st order phase transition

Discussion

- Consistency with fpeak-Lambda relation points to

  - purely baryonic EoS

  - (or an at most weak phase transition → no strong compactification)

  in the tested (!) density regime

- fpeak also determines maximum density in postmerger remnant

- postmerger GW emission provides complimentary information to inspiral

  → probes higher density regime

Bauswein et al. 2018

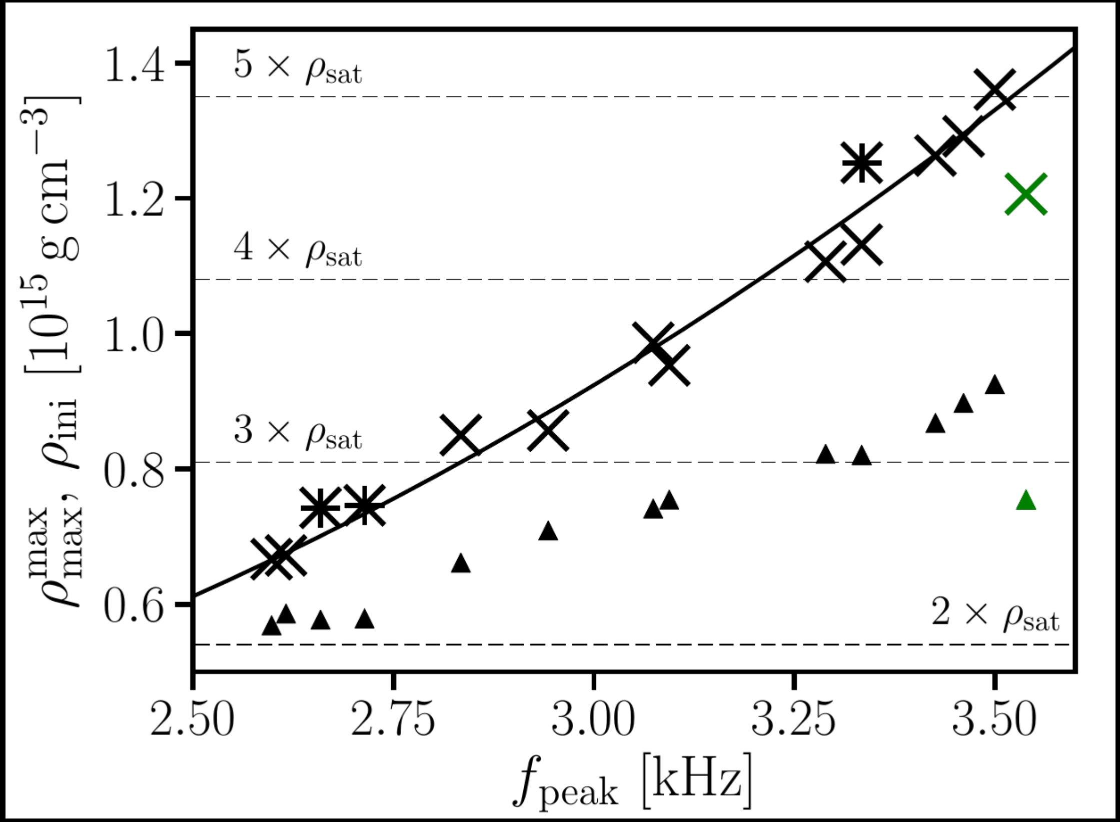

Probed densities / NS masses

- Dots: NS mass with central density = maximum density during early postmerger evolution

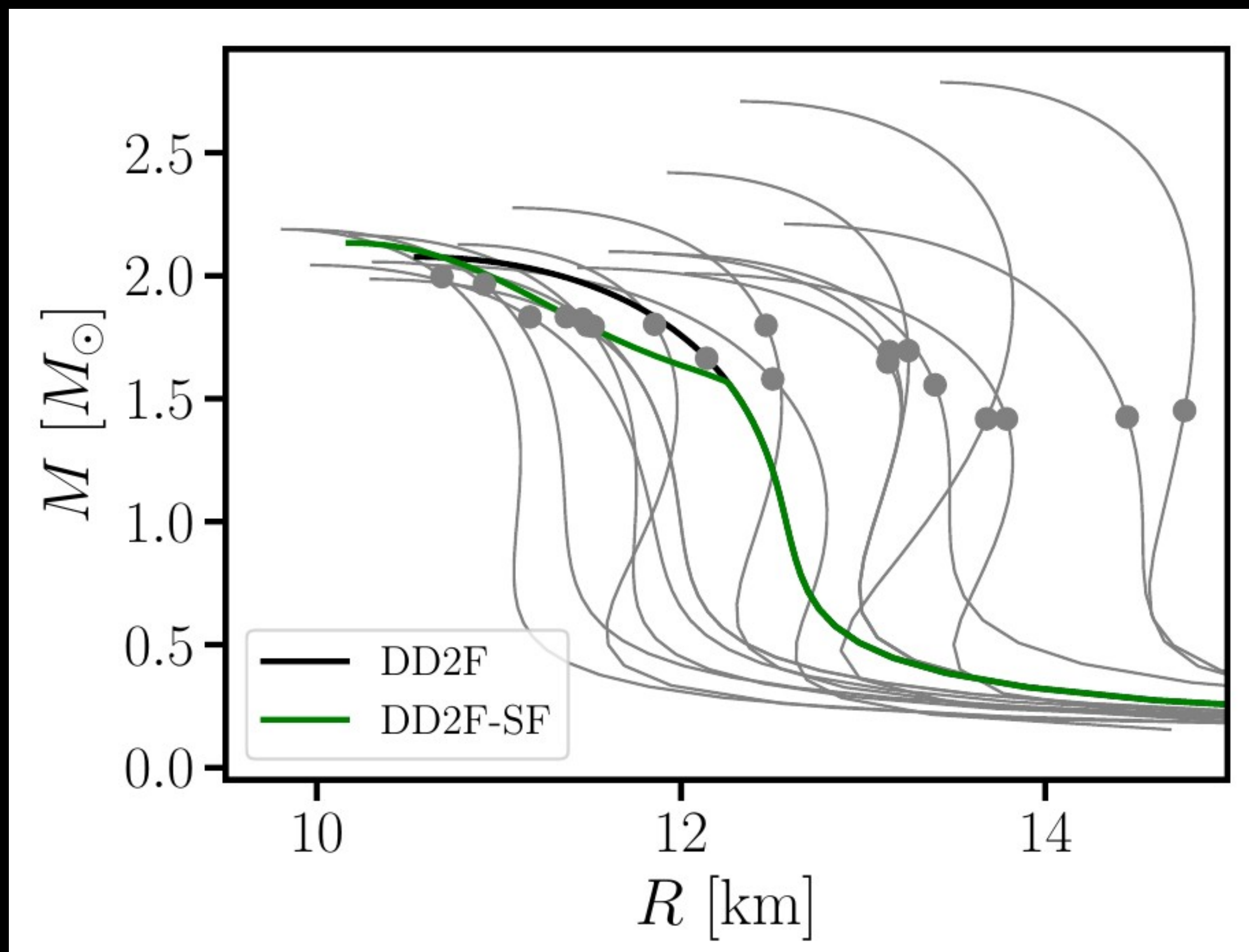

For 1.35-1.35 Msun merger – higher binary masses probe higher densities / NS masses

Conclusions

- NS radius must be larger than 10.7 km (very robust)
- More stringent constraints from future detections
- NS radius measurable from dominant postmerger frequency
- Explicitly shown by GW data analysis
- Threshold binary mass for prompt collapse → maximum mass M_{max}
- Strong 1st order phase transitions leave characteristic imprint on GW (psotmerger frequency higher than expected from inspiral)
- Complementarity of inspiral and postmerger phase → postmerger probes higher density regime